Thioamide Quenching of Fluorescent Probes through Photoinduced Electron Transfer: Mechanistic Studies and Applications

Jacob M. Goldberg, Solongo Batjargal, Benson S. Chen, and E. James Petersson

Department of Chemistry, University of Pennsylvania
231 South 34th Street, Philadelphia, Pennsylvania 19104-6323 USA.

General Information. Boc-L-thionoleucine-1-(6-nitro)benzotriazolide, Boc-L-thionoalanine-1-(6-nitro)benzotriazolide, and 5-carboxyfluorescein were purchased from Bachem (Torrance, CA, USA). Fmoc-Ala-OH, Fmoc-Asn(Trt)-OH, Fmoc-Asp(OtBu)-OH, Fmoc-Cys(Trt)-OH, Fmoc-Glu(OtBu)-OH, Fmoc-Gln(Trt)-OH, Fmoc-Gly-OH, Fmoc-Lys(Boc)-OH, Fmoc-Met-OH, Fmoc-Phe-OH, Fmoc-Pro-OH, Fmoc-Ser(OtBu)-OH, Fmoc-Tyr(OtBu)-OH, Fmoc-Val-OH, 2-chlorotrityl resin, and 2-(1*H*-benzotriazol-1-yl)-1,1,3,3-tetramethyluronium hexafluorophosphate (HBTU) were purchased from Novabiochem (currently EMD Millipore; Billerica, MA, USA). A "CyDye™ Post-Labeling Reactive Dye Pack" containing mono-reactive, *N*-hydroxysuccinimide activated Cy3 and Cy5 dyes was purchased from Amersham Biosciences (currently GE Healthcare; Pittsburgh, PA, USA). Acridine orange was purchased from Calbiochem (currently EMD Millipore). Coumarin 102, 4-chloro-7-nitro-1,2,3-benzoxadiazole

(NBD-chloride), fluorescein-5-isothiocyanate, rhodamine 6G chloride, resorufin sodium salt, ATTO 655, Sigmacote®, *N*,*N*-diisopropylethylamine (DIPEA), piperidine, and tris(2-carboxyethyl)phosphine hydrochloride (TCEP) were purchased from Sigma-Aldrich (St. Louis, MO, USA). Glass peptide synthesis reaction vessels (RVs) were treated with Sigmacote® prior to use. Alexa Fluor® 488 carboxylic acid, succinimidyl ester (as a mixture of isomers); Texas Red® hydrazide, > 90% single isomer; BODIPY® R6G, succinimidyl ester; and BODIPY® FL, succinimidyl ester were purchased from Life Technologies (Grand Island, NY, USA). Ethanolamine was purchased from Riedel-de Haën (Seelze near Hannover, Germany; currently Sigma-Aldrich). Fluorescein-5-maleimide was purchased from Promega (Madison, WI, USA). All other chemical reagents were purchased from Fisher Scientific (Pittsburgh, PA, USA). A QuickChange® site-directed mutagenesis kit, *E. coli* BL21(DE3) cells, and all restriction enzymes were purchased from Stratagene (currently Agilent Technologies; Santa Clara, CA, USA). Ni-NTA resin and a QIAquick gel extraction kit were purchased from Qiagen (Valencia, CA, USA). DNA oligomers were purchased from Integrated DNA Technologies, Inc. (Coralville, IA, USA). DNA sequencing was performed at the University of Pennsylvania DNA sequencing facility. Milli-Q filtered (18 MΩ) water was used for all solutions (currently EMD Millipore). UV absorbance spectra were obtained with a Hewlett-Packard 8452A diode array spectrophotometer (currently Agilent Technologies). Fluorescence spectra were collected with a Varian Cary Eclipse fluorescence spectrophotometer fitted with a Peltier multicell holder (currently Agilent Technologies). Protein fluorescence lifetime measurements were made using a Photon Technology International (PTI) QuantaMaster™ 40 fluorescence spectrometer (Birmingham, NJ, USA). Matrix-assisted laser desorption ionization (MALDI) mass spectra were collected with a Bruker Microflex LRF MALDI-TOF mass spectrometer for small peptides and a Bruker Ultraflex III MALDI-TOF-TOF mass spectrometer for proteins (Billerica, MA,

USA). "High resolution" ESI mass spectrometry (HRMS) was conducted with a Waters LCT Premier XE LC/MS (Milford, MA, USA). Peptides and fluorescent conjugates were purified with a Varian ProStar High-Performance Liquid Chromatography (HPLC, currently Agilent Technologies) instrument outfitted with a diode array detector using linear solvent gradients consisting of an aqueous phase (H_2O + 0.1% CF_3CO_2H) and organic phase (CH_3CN + 0.1% CF_3CO_2H). Protein purification was conducted on an ÄKTA fast protein liquid chromatography (FPLC) system (GE Healthcare Life Sciences; Piscataway Township, NJ, USA). Gels were imaged using a Typhoon FLA 7000 (GE Healthcare Life Sciences).

Synthesis of Small Molecule Fluorophores.

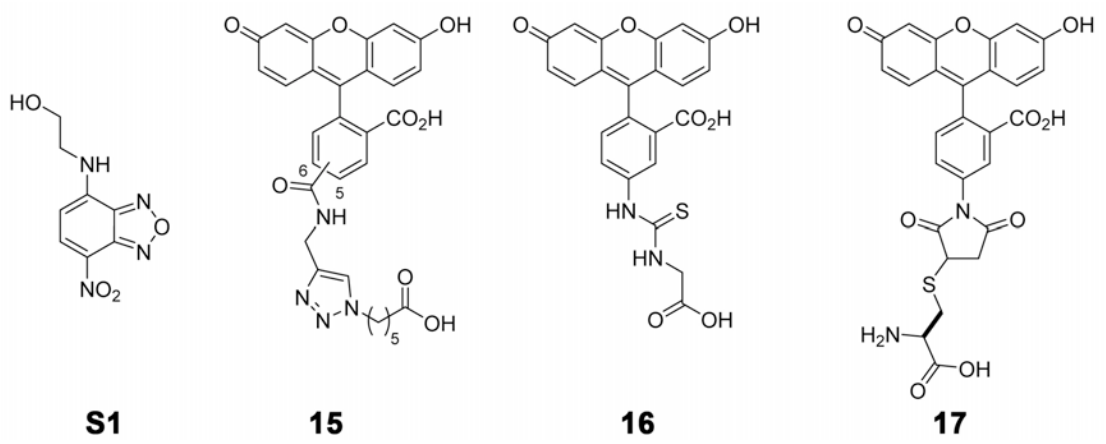

Figure S1. Structures of Fluorophore Conjugates.

2-((7-nitrobenzo[*c*][1,2,5]oxadiazol-4-yl)amino)ethanol (NBD-ethanolamine, S1). Ethanolamine (0.0604 mL, 1 mmol) was added dropwise to a stirred solution of NBD-chloride (0.293 g. 1.2 mmol) and triethylamine (0.1673 mL, 1.2 mmol) in anhydrous CH_2Cl_2 (10 mL). The solution was allowed to stir overnight in the dark. The product was purified to homogeneity by reverse-phase HPLC on a Prodigy 5 µm ODS-2 analytical C18 column (Phenomenex; Torrance, CA) using a linear solvent gradient that ranged from 99% to 98% aqueous phase over 10 min, then to 68% aqueous phase over 20 min, then to 0% aqueous phase over 20 min, then

returning to 98% aqueous phase during a 10 min wash out period. Using this method, the product eluted at 31.5 min. HRMS (ESI) m/z calcd for $C_8H_7N_4O_4^-$ $[M-H]^-$ 223.0467, found 223.0474.

5- and 6-(((1-(5-carboxypentyl)-1*H*-1,2,3-triazol-4-yl)methyl)carbamoyl)-2-(6-hydroxy-3-oxo-3*H*-xanthen-9-yl)benzoic acid (Fam-Click, 15). Fluorescein 5- and 6-proparglyamide (Fluorescein-alkyne) and Tris-(3-hydroxypropyltriazolylmethyl)amine (THPTA) were synthesized as described previously.[1] Aqueous solutions of sodium ascorbate (100 mM), THPTA (50 mM), fluorescein alkyne (0.8 mM) and copper sulfate (80 mM) were prepared immediately prior to use. The copper sulfate (1.25 µL, 100 nmol), THTPA (10 µL, 500 nmol), and sodium ascorbate solutions (6 µL, 600 nmol) were thoroughly mixed in a microcentrifuge tube and allowed to stand for 5 min. The resulting solution (17.25 µL) was then added to a microcentrifuge tube containing 6-azidohexanoic acid (31.4 µL, ~200 nmol) and the fluorescein alkyne solution (250 µL, 200 nmol) in phosphate-buffered saline (691.35 µL; 12 mM NaH_2PO_4, 50 mM NaCl, 4.7 mM KCl, pH 8.00). An additional aliquot of aqueous sodium ascorbate (10 µL, 1000 nmol) was added to the microcentrifuge tube and the contents were mixed thoroughly. The reaction was allowed to proceed at room temperature in the dark overnight. The resulting product was purified by HPLC using the same gradient described for compound **S1**. Using this method, the product eluted at 36.5 min. HRMS (ESI) m/z calcd for $C_{30}H_{25}N_4O_8^-$ $[M-H]^-$ 569.1672, found 569.1650; m/z calcd for $C_{30}H_{27}N_4O_8^+$ $[M+H]^+$ 571.1829, found 571.1830.

5-(3-(carboxymethyl)thioureido)-2-(6-hydroxy-3-oxo-3H-xanthen-9-yl)benzoic acid (FITC, 16). Fluorescein-5-isothiocyanate (FITC; 0.5 mg, 1.28 µmol) was dissolved in 50 µL dimethyl sulfoxide. This solution was then slowly added to a solution of glycine (10 mg, 133 µmol) in sodium bicarbonate buffer (1.00 mL; 0.1 M, pH 9.00) with mild vortexing. The reaction was allowed to proceed overnight in the dark at room temperature. The product was

purified by HPLC using the same gradient described for compound **S1**. Using this method, the product eluted at 36.8 min. HRMS (ESI) m/z calcd for $C_{23}H_{17}N_2O_7S^+$ $[M+H]^+$ 465.0756, found 465.0745.

5-(3-((2-amino-2-carboxyethyl)thio)-2,5-dioxopyrrolidin-1-yl)-2-(6-hydroxy-3-oxo-3H-xanthen-9-yl)benzoic acid (Fam-Cys, ψ, 17). Fluorescein-5-maleimide (100 µg, 234 nmol) was dissolved in 23 µL dimethyl sulfoxide. This solution was then slowly added to a solution of cysteine (0.08 mg, 660 nmol) in sodium phosphate buffer (200 µL; 10 mM, pH 7.00). The reaction was allowed to proceed overnight in the dark at room temperature. The product was purified by HPLC using the same gradient described for compound **S1**. Using this method, the product eluted at 35.4 min. HRMS (ESI) m/z calcd for $C_{27}H_{21}N_2O_9S^+$ $[M+H]^+$ 549.0968, found 549.0953.

Small Peptide Synthesis and Purification. The peptides LP_2C, $L'P_2C$, LG_2C, $L'G_2C$, LP_3C, $L'P_3C$, LG_3C, $L'G_3C$, AAFKGC, and A'AFKGC (n.b., the prime symbol ' indicates a thioamide bond) were each synthesized on a 12.5 µmol scale on 2-cholortrityl resin using standard techniques. Since the first several amino acid couplings in the oxo- and thiopeptides are identical, these residues were coupled on a 25 µmol scale in a common pot for each pair of peptides. The resin was then divided into two equal portions for the final amino acid coupling of either Ala, Ala', Leu or Leu' and the reagents were scaled accordingly. For a typical synthesis, 2-chlorotrityl resin (100-200 mesh; 0.6 mmol substitution/g; 25 µmol) was added to a dry reaction vessel (RV). Two successive 15 min incubations with 5 mL dimethylformamide (DMF) and magnetic stirring were used to swell the resin. After swelling, DMF was removed with vacuum suction. The first amino acid in DMF (5 equiv; 83 mM, 1.5 mL) and DIPEA (10 equiv; 44 µL) was added to the RV and the mixture was allowed to react for 30 min with magnetic stirring. Spent solution was removed with vacuum suction and the resin beads were washed thoroughly

with DMF. Excess DMF was removed with vacuum suction and the resin beads were deprotected by treatment with 20% piperidine in DMF (5 mL) for 20 min with magnetic stirring. The deprotection solution was drained from the RV and the beads were rinsed extensively with DMF. Subsequent amino acid couplings and deprotections proceeded as described above, with the exception that the remaining Fmoc-protected amino acids were activated with HBTU (5 equiv) prior to addition to each reaction. Since thioalanine and thioleucine were introduced through the pre-activated Boc-L-thionoalanine-1-(6-nitro)benzotriazolide or Boc-L-thionoleucine-1-(6-nitro)benzotriazolide, HBTU was not added for these couplings. The final N-terminal Fmoc group was removed from the oxo peptides before cleavage from the resin. After the beads were washed extensively with DMF and dried with CH_2Cl_2, peptides were cleaved by successive 60 min and 30 min incubations on a rotisserie with 2.5 mL of a fresh cleavage cocktail of trifluoroacetic acid (TFA), water, and triisopropylsilane (TIPS) (10:9:1 v/v). After each treatment, the resulting solution was expelled from the RV with nitrogen, reduced to a volume of less than 1 mL by rotary evaporation, and diluted with 6 mL of CH_3CN/H_2O (2:1 v/v).

All small peptides were purified to homogeneity by reverse-phase HPLC on a Vydac 218TP C18 semi-prep column (Grace/Vydac; Deerfield, IL) using linear solvent gradients consisting of an aqueous phase (H_2O + 0.1% CF_3CO_2H) and organic phase (CH_3CN + 0.1% CF_3CO_2H). For the glycine and proline peptides, the gradient was isocratic at 98% aqueous phase for 6 min and then ranged from 98% to 60% aqueous phase over 19 min, then to 0% aqueous phase over 5 min, then returning to 98% aqueous phase during a 10 min wash out period. For the AAFKGC peptides, the gradient was isocratic at 98% aqueous phase for 4 min and then ranged from 98% to 80% aqueous phase over 3 min, then to 71% aqueous phase over 9 min, then to 0% aqueous phase over 4 min, then returning to 98% aqueous phase during a 10 min wash out period.

MALDI MS was used to confirm identities (Table S1). Purified peptides were dried in a vacuum centrifuge (Savant/Thermo Scientific; Rockford, IL, USA).

Peptides were labeled with 5-fluorescein maleimide using the following procedure. Dry peptides were reconstituted in 20 mM sodium phosphate (1 mL, pH 7.0) in microcentrifuge tubes. An aliquot (10 µL) of Bond-Breaker 0.5 M TCEP solution, Neutral pH (Thermo Scientific Pierce) was added to each tube and the tubes were vortexed lightly. A solution of fluorescein maleimide (0.25 mg in 25 µL dimethyl sulfoxide) was added to each tube and the tubes were vortexed briefly and allowed to sit at room temperature for 4 h and overnight at 4 °C. The peptides were purified to homogeneity by reverse-phase HPLC using the same methods described above. MALDI MS was used to confirm identity (Table S1). Purified peptides were dried in a vacuum centrifuge.

Table S1. Calculated and Observed Small Peptide Masses.

Peptide	Calculated $[M+H]^+$	Observed $[M+H]^+$	Calculated $[M+Na]^+$	Observed $[M+Na]^+$
LP_2C	429.22	429.40	451.20	451.38
$L'P_2C$	445.19	445.20	467.18	467.18
LP_2C-Fam ($LP_2\psi$)	856.29	856.22	878.27	878.19
$L'P_2C$-Fam ($L'P_2\psi$)	872.26	872.17	894.24	894.15
LG_2C	349.15	349.20	371.14	371.19
$L'G_2C$	365.13	365.17	387.11	387.16
LG_2C-Fam ($LG_2\psi$)	776.22	776.11	798.21	798.08
$L'G_2C$-Fam ($L'G_2\psi$)	792.20	792.11	814.18	814.09
LP_3C	526.27	526.15	548.25	548.13
$L'P_3C$	542.25	542.26	564.23	564.24
LP_3C-Fam ($LP_3\psi$)	953.54	953.28	975.32	975.25
$L'P_3C$-Fam ($L'P_3\psi$)	969.32	969.25	991.30	991.23
LG_3C	406.18	406.08	428.16	428.08
$L'G_3C$	422.15	422.05	444.13	444.04
LG_3C-Fam ($LG_3\psi$)	833.24	833.26	855.23	855.27
$L'G_3C$-Fam ($L'G_3\psi$)	849.22	849.23	871.20	871.19
AAFKGC	596.29	596.80	618.27	618.78
A'AFKGC	612.26	612.59	634.25	634.56
AAFKGψ	1023.36	1023.83	1045.34	1045.67
A'AFKGC-Fam (A'AFKGψ)	1039.33	1039.57	1061.31	1061.57

Small Molecule Fluorescence Spectroscopy. Fluorescence measurements in the presence and absence of 50 mM acetamide or 50 mM thioacetamide were conducted for each fluorophore in 100 mM sodium phosphate buffer, pH 7.00. Fluorophores were used as supplied by the manufacturer without further purification. Concentrated stocks of each fluorophore in buffer were prepared immediately prior to use, with the exception of Alexa Fluor 488, BODIPY FL, BODIPY R6G, Cy3, and Cy5. Concentrated stocks of these dyes were prepared one day prior to use to allow the succinimidyl esters to hydrolyze. A minimal amount of spectroscopic grade ethanol was added to the BODIPY R6G sample to aid in dissolution. Compounds **S1** and **15**-**17** were used to prepare concentrated stocks of the NBD and fluorescein conjugates, as appropriate.

For each fluorophore, samples were prepared by diluting the concentrated stock with additional buffer and 100 mM solutions of acetamide or thioacetamide in buffer such that all solutions of a given fluorophore were equimolar in concentration. Steady-state fluorescence spectra were collected as the average of three scans at 25 °C of three samples of each solution using quartz fluorometer cells with path lengths of 1.00 cm. Excitation wavelengths are given in the captions to Figures S2 – S17. The excitation and emission slit widths were 5 nm, the scan rate 120 nm/min, the averaging time 0.500 s, and the data interval 1.0 nm. Representative spectra are shown in Figures S2 – S17. The steady-state quenching efficiency, E_Q (SS), of aqueous thioacetamide was calculated using Equation S1.

$$E_Q(\mathrm{SS}) = 1 - (F/F_0) \qquad \text{(S1)}$$

In this equation, F_0 is the fluorescence intensity of the fluorophore at the wavelength of maximum emission in 100 mM phosphate buffer and F is the corresponding fluorescence intensity at the same wavelength in 50 mM thioacetamide. The E_Q values reported in Table 1 are the average of three trials.

Small Molecule Fluorescence Lifetime Measurements. Time-resolved fluorescence measurements were performed on freshly prepared samples using the Time-Correlated Single Photon Counting (TCSPC) method. The TCSPC system consisted of a blue diode laser (PicoQuant GmbH; Berlin, Germany) generating 10 MHz output pulses at 405 nm, a subtractive double monochromator with an MCP-PMT (Hamamatsu Photonics R2809U; Bridgewater, NJ), and a TCSPC computer board (Becker and Hickl SPC-630; Berlin, Germany). Emission was monitored at the wavelength of maximum fluorescence. Data analysis was performed with FluoFit software (Picoquant) using an exponential decay model (Eq. S2).

$$I(t) = \sum_{i=1}^{n} A_i e^{-\frac{t}{\tau_i}} \qquad \text{(S2)}$$

Here, the parameters A_i and τ_i are the amplitude and lifetime of the i^{th} component, respectively. Reduced χ^2 values were calculated for each fit according to Equation S3.

$$\chi^2 = \frac{1}{N-p}\sum_{j=1}^{N} W(j)^2\left[decay(j) - fit(j)\right]^2 \qquad W(j) = \frac{1}{\sqrt{decay(j)}} \qquad \text{(S3)}$$

In this equation, N is the number of fitted data points j (i.e. measured photon counts at a given delay time, a bin); p is the number of adjustable, fitted parameters; $W(j)$ is a Poisson weighting factor; $decay(j)$ is the experimentally determined decay curve; and $fit(j)$ is the fitted model. Weighted residuals were calculated according to Equation S4 using these values.

$$R = W(j)\left[decay(j) - fit(j)\right] \qquad \text{(S4)}$$

Lifetime decays of all of the fluorophores could be fit using a single-exponential model (Eq. S2, $n = 1$) with the exception of those of the FITC (**16**) and the Fam-Cys (**17**) conjugates. For these samples, a bi-exponential model (Eq. S2, $n = 2$) was more appropriate as judged by χ^2 analysis

and inspection of the weighted-residual plots. Representative fits, the corresponding residual plots, χ^2-analyses, and lifetimes are presented in Figures S2 – S17.

For FITC in buffer (Fig. S6), we found long (τ_1 = 3.67 ± 0.02 ns; 81% by amplitude, 92% by intensity) and short (τ_2 = 1.32 ± 0.09 ns; 19% by amplitude, 8% by intensity) lifetime components that accounted for the observed trace. Both components were quenched in the presence of 50 mM thioacetamide (τ_1 = 2.38 ± 0.01 ns; 75.8% by amplitude, 88.6% by intensity and τ_2 = 0.96 ± 0.05 ns; 24.2% by amplitude, 11.4% by intensity). For the Fam-Cys conjugate we found τ_1 = 3.78 ± 0.02 ns (87.9% by amplitude; 95.5% by intensity) and τ_2 = 1.29 ± 0.14 ns (12.1% by amplitude; 4.5% by intensity) in buffer (Fig. S7). In the presence of 50 mM thioacetamide we found τ_1 = 2.58 ± 0.01 ns (63.5% by amplitude; 76.3% by intensity) and τ_2 = 1.39 ± 0.03 ns (36.5% by amplitude; 23.7% by intensity).

Quenching efficiencies based on lifetime data, $E_Q(\tau)$, were calculated by comparing the fluorescence lifetimes of each fluorophore in buffer (τ_0) and in 50 mM thioacetamide (τ_{Thio}) using Equation S5.

$$E_Q(\tau) = 1 - (\tau_{Thio}/\tau_0) \qquad \text{(S5)}$$

Since accurately parsing the importance of the relative thioacetamide quenching efficiencies of the various components each of the bi-exponential fits is difficult, we calculated $E_Q(\tau)$ from the intensity-weighted average lifetimes of the FITC-glycine and fluorescein maleimide-cysteine in buffer ($\tau_{avg,0}$) and 50 mM thioacetamide (τ_{avg}) using Equation S5.

Small Molecule Absorbance Spectroscopy. UV-visible spectra were acquired of dilute ($A_{\lambda ex} \approx 0.10$) and concentrated solutions of each fluorophore in 100 mM sodium phosphate buffer, pH 7.00; in 50 mM thioacetamide; and in 50 mM acetamide in quartz cells with 1.00 cm path lengths. No difference was observed between the background-corrected, visible portion of the

spectra of solutions that contained thioacetamide and those that did not. This observation suggests that the fluorophores and thioacetamide do not form ground-state complexes with unusual optical characteristics, which would have been indicative of a static-quenching mechanism. Since the absorbance spectrum of 50 mM thioacetamide overlaps slightly with that of coumarin-102, a difference spectrum (the spectrum of 50 mM thioacetamide subtracted from the spectrum of coumarin-102 in 50 mM thioacetamide) was used to facilitate this comparison (Fig. S2). Representative absorbance spectra of each dye in buffer, 50 mM thioacetamide, and 50 mM acetamide are shown in Figures S2 – S17. Fluorophore concentrations were determined using previously published extinction coefficients, which are given in the captions to Figures S2-S17.

Molecular Volume Calculations. The ground-state geometries of each fluorophore were optimized at the AM1 level and the molecular volume was calculated using Spartan (Wavefunction, Inc.; Irvine, CA). Reactive handles were not included in these calculations to give a better comparison of the contribution of the fluorescent moiety, even though the tethers can be quite large. The results of these calculations are summarized in Table 1. Space-filling models are shown in Figures S2 – S17, as appropriate.

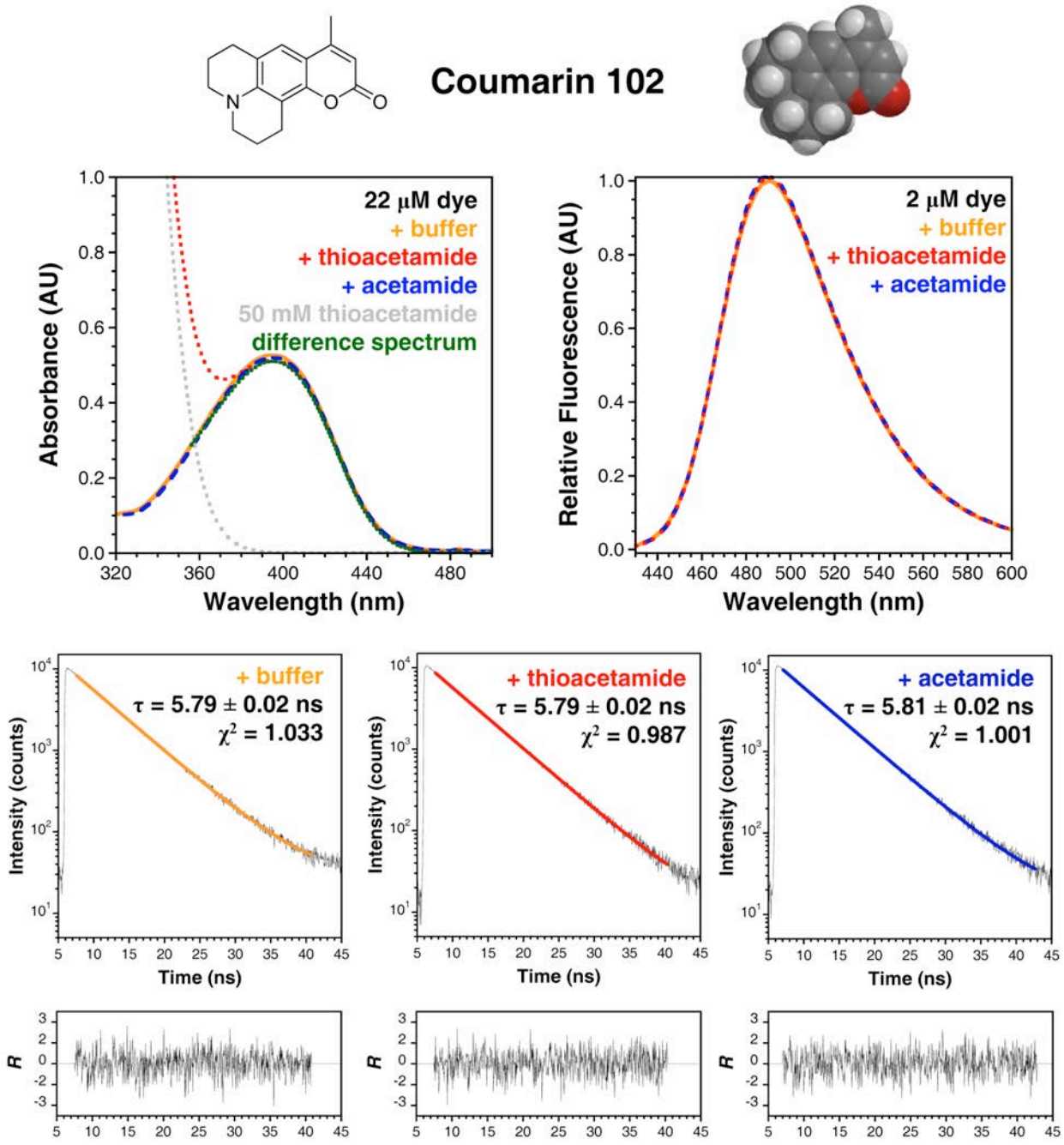

Figure S2. Coumarin 102 (**4**). Chemical structure and space-filling model of coumarin 102. Background-corrected absorbance and normalized fluorescence (λ_{ex} = 393 nm) spectra of the dye in 100 mM phosphate buffer, pH 7.00 (solid orange trace), 50 mM acetamide (dashed blue trace), and 50 mM thioacetamide (dotted red trace). The absorbance spectrum of 50 mM thioacetamide (gray dotted trace) and the corresponding difference spectrum (dotted green trace; "dye + thioacetamide" – "50 mM thioacetamide) are shown for comparison. Single-exponential fits and weighted residuals of fluorescence lifetime measurements of the dye in buffer, 50 mM thioacetamide, and 50 mM acetamide. Concentration calculated from $\varepsilon_{387\ nm}$ = 23,000 M^{-1}•cm^{-1}.[2]

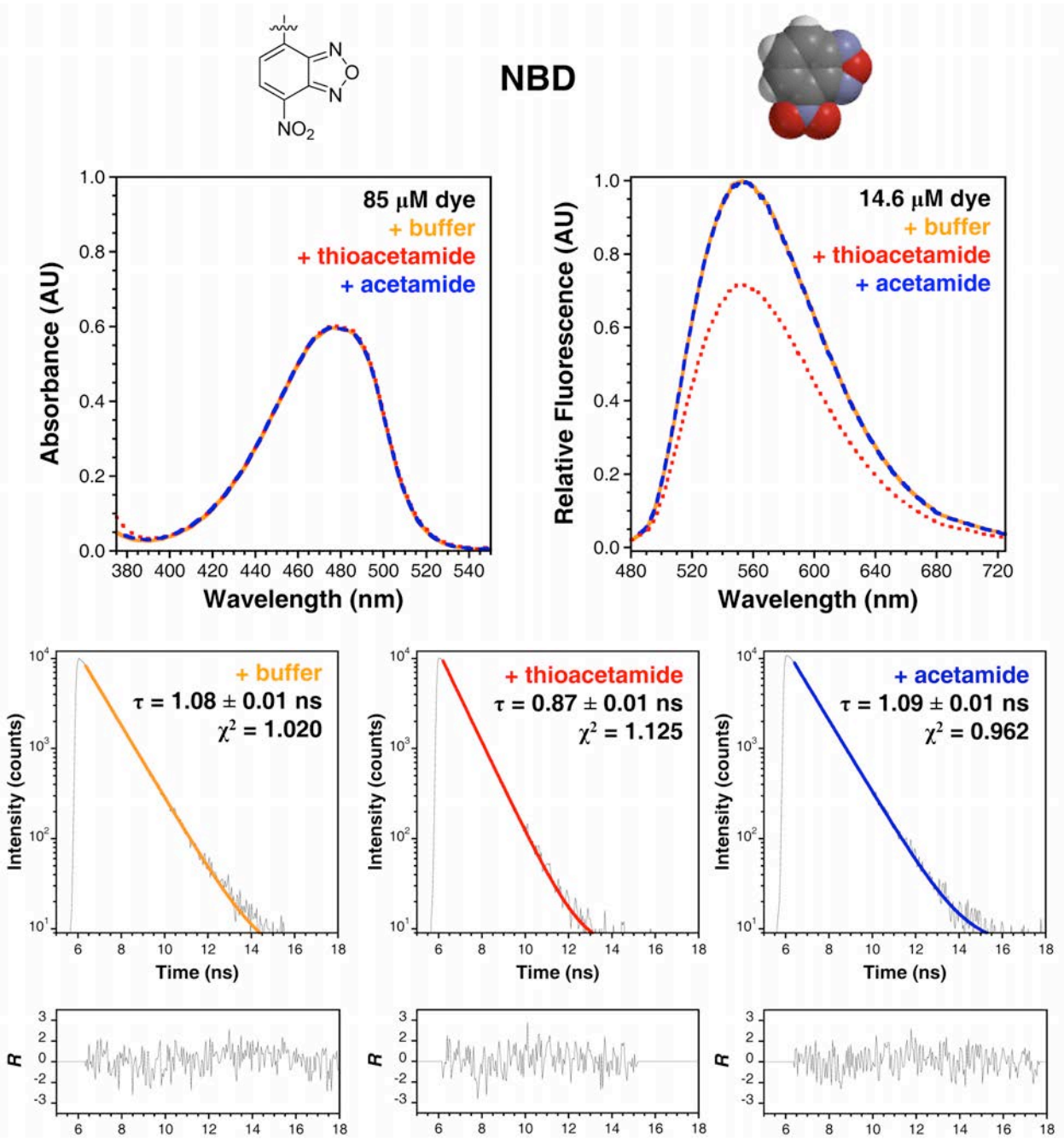

Figure S3. NBD (**2**, **S1**). Chemical structure and space-filling model of NBD. Background-corrected absorbance and normalized fluorescence (λ_{ex} = 460 nm) spectra of NBD-ethanolamine (**S1**) in 100 mM phosphate buffer, pH 7.00 (solid orange trace), 50 mM acetamide (dashed blue trace), and 50 mM thioacetamide (dotted red trace). Single-exponential fits and weighted residuals of fluorescence lifetime measurements of the dye in buffer, 50 mM thioacetamide, and 50 mM acetamide. Concentration calculated from $\varepsilon_{484\ nm}$ = 6,835 M^{-1}•cm^{-1}.[3]

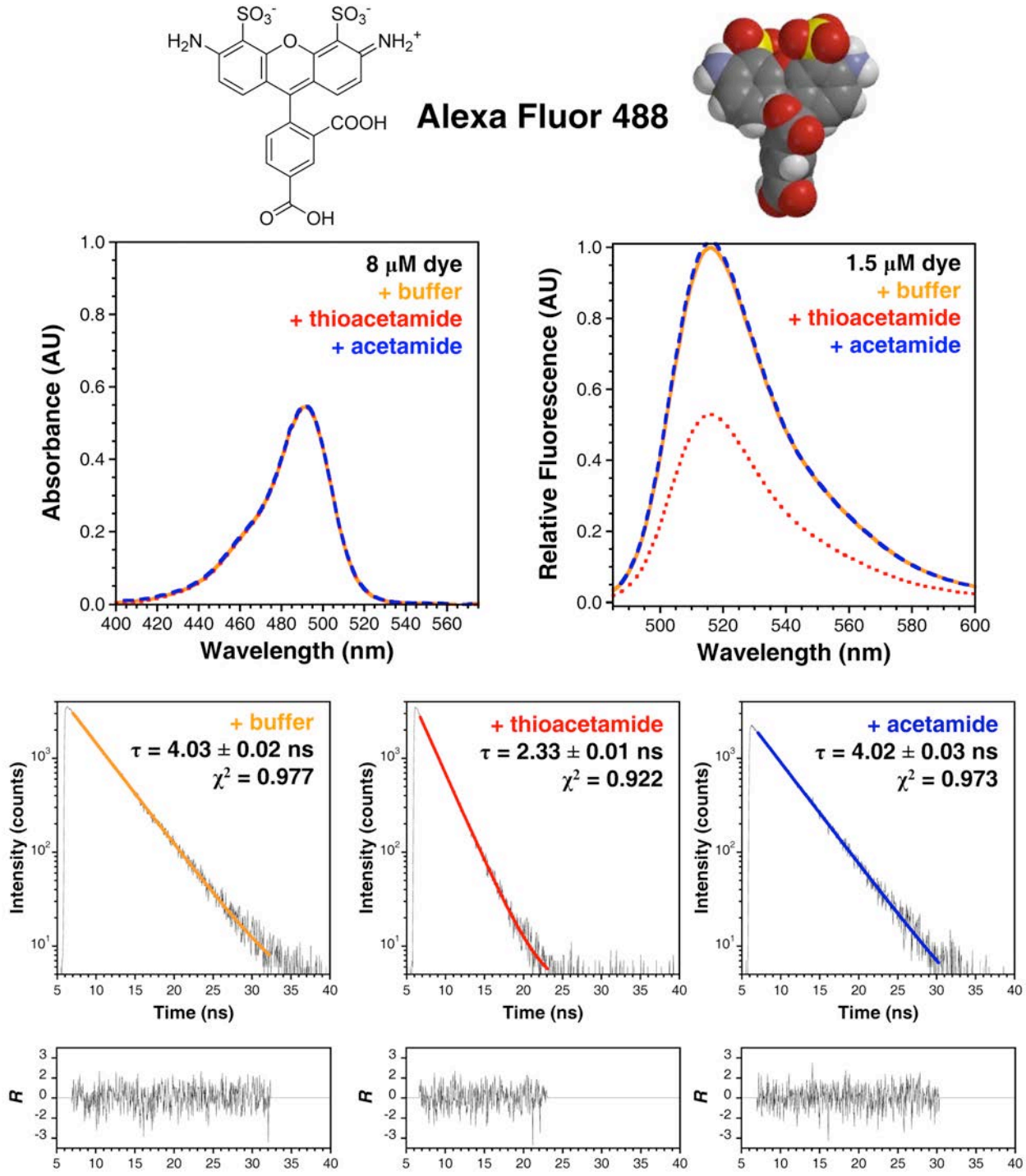

Figure S4. Alexa Fluor 488 (**14**). Chemical structure and space-filling model of Alexa Fluor 488. Background-corrected absorbance and normalized fluorescence (λ_{ex} = 475 nm) spectra of the dye in 100 mM phosphate buffer, pH 7.00 (solid orange trace), 50 mM acetamide (dashed blue trace), and 50 mM thioacetamide (dotted red trace). Single-exponential fits and weighted residuals of fluorescence lifetime measurements of the dye in buffer, 50 mM thioacetamide, and 50 mM acetamide. Concentration calculated from $\varepsilon_{495\ nm}$ = 71,000 M^{-1}•cm^{-1}.[4]

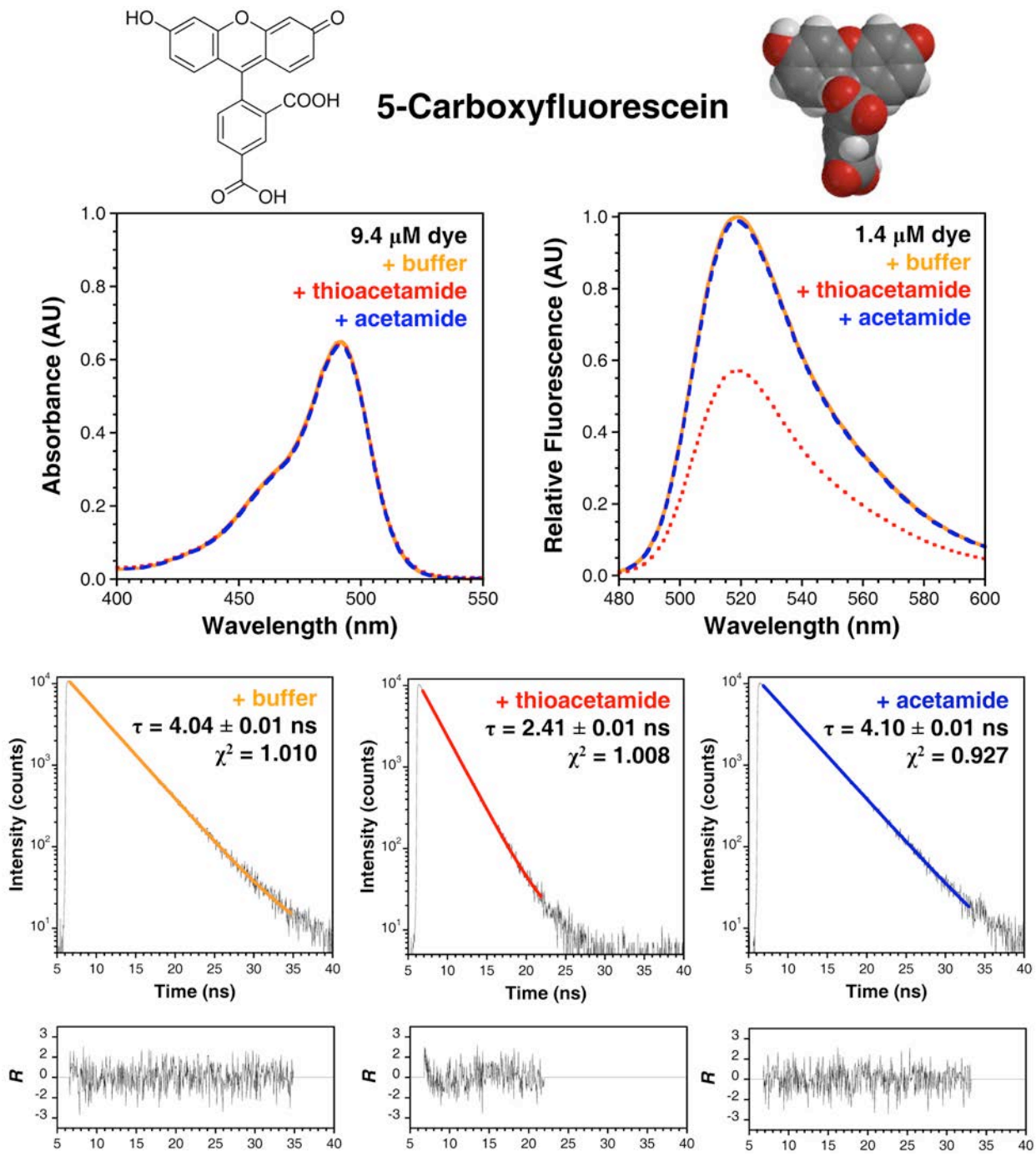

Figure S5. 5-Carboxyfluorescein (**12**). Chemical structure and space-filling model of 5-carboxyfluorescein. Background-corrected absorbance and normalized fluorescence (λ_{ex} = 470 nm) spectra of the dye in 100 mM phosphate buffer, pH 7.00 (solid orange trace), 50 mM acetamide (dashed blue trace), and 50 mM thioacetamide (dotted red trace). Single-exponential fits and weighted residuals of fluorescence lifetime measurements of the dye in buffer, 50 mM thioacetamide, and 50 mM acetamide. Concentration calculated from $\varepsilon_{494\ nm}$ = 68,000 M^{-1}•cm^{-1}.[5]

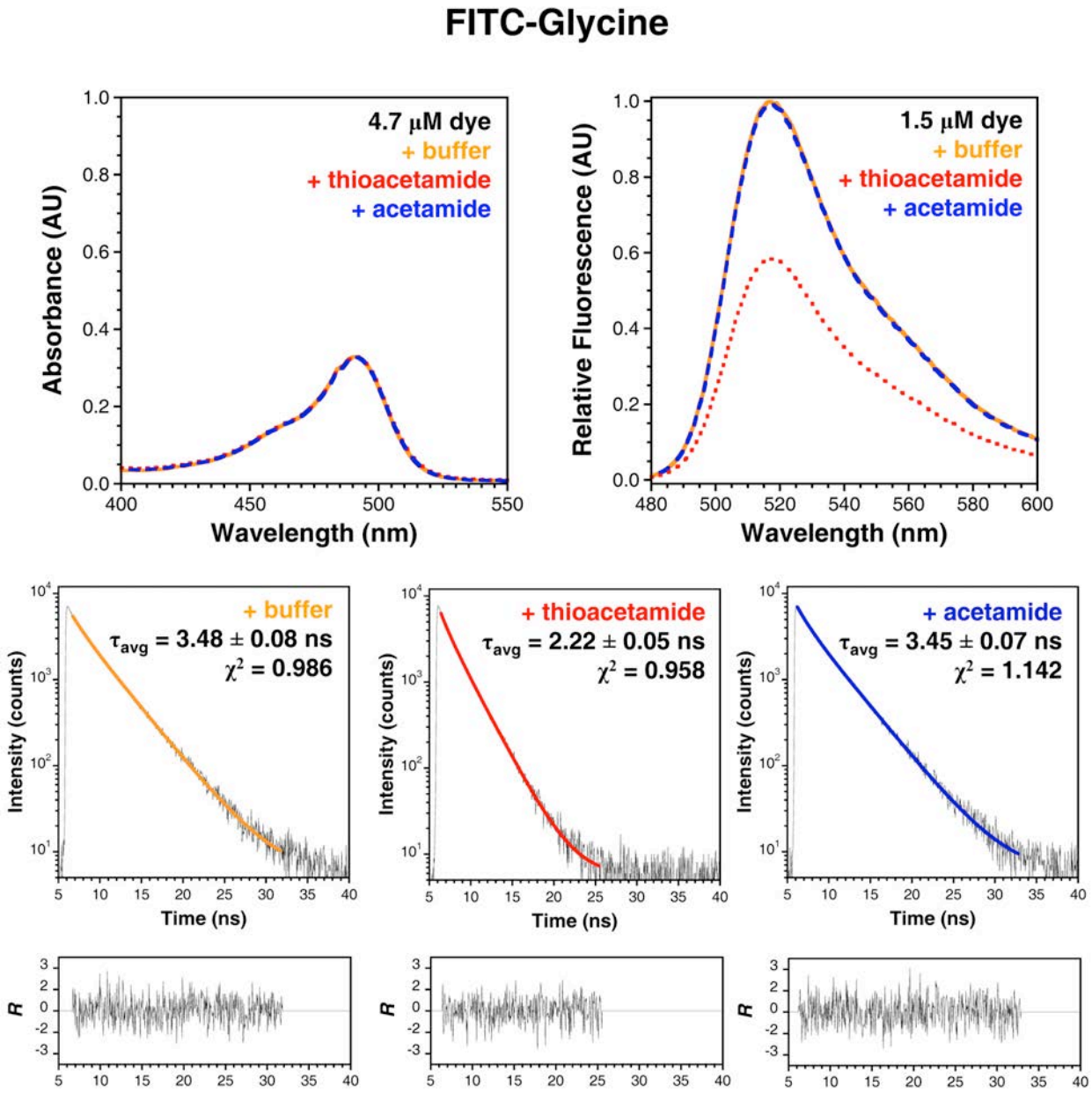

Figure S6. FITC-Glycine (**16**). Background-corrected absorbance and normalized fluorescence (λ_{ex} = 450 nm) spectra of the FITC conjugate (**16**) in 100 mM phosphate buffer, pH 7.00 (solid orange trace), 50 mM acetamide (dashed blue trace), and 50 mM thioacetamide (dotted red trace). Bi-exponential fits and weighted residuals of fluorescence lifetime measurements of the dye in buffer, 50 mM thioacetamide, and 50 mM acetamide. Reported lifetimes (τ_{avg}) are intensity-weighted averages of the long and short components. Concentration calculated from $\varepsilon_{494\ nm}$ = 68,000 M^{-1}•cm^{-1}.[5]

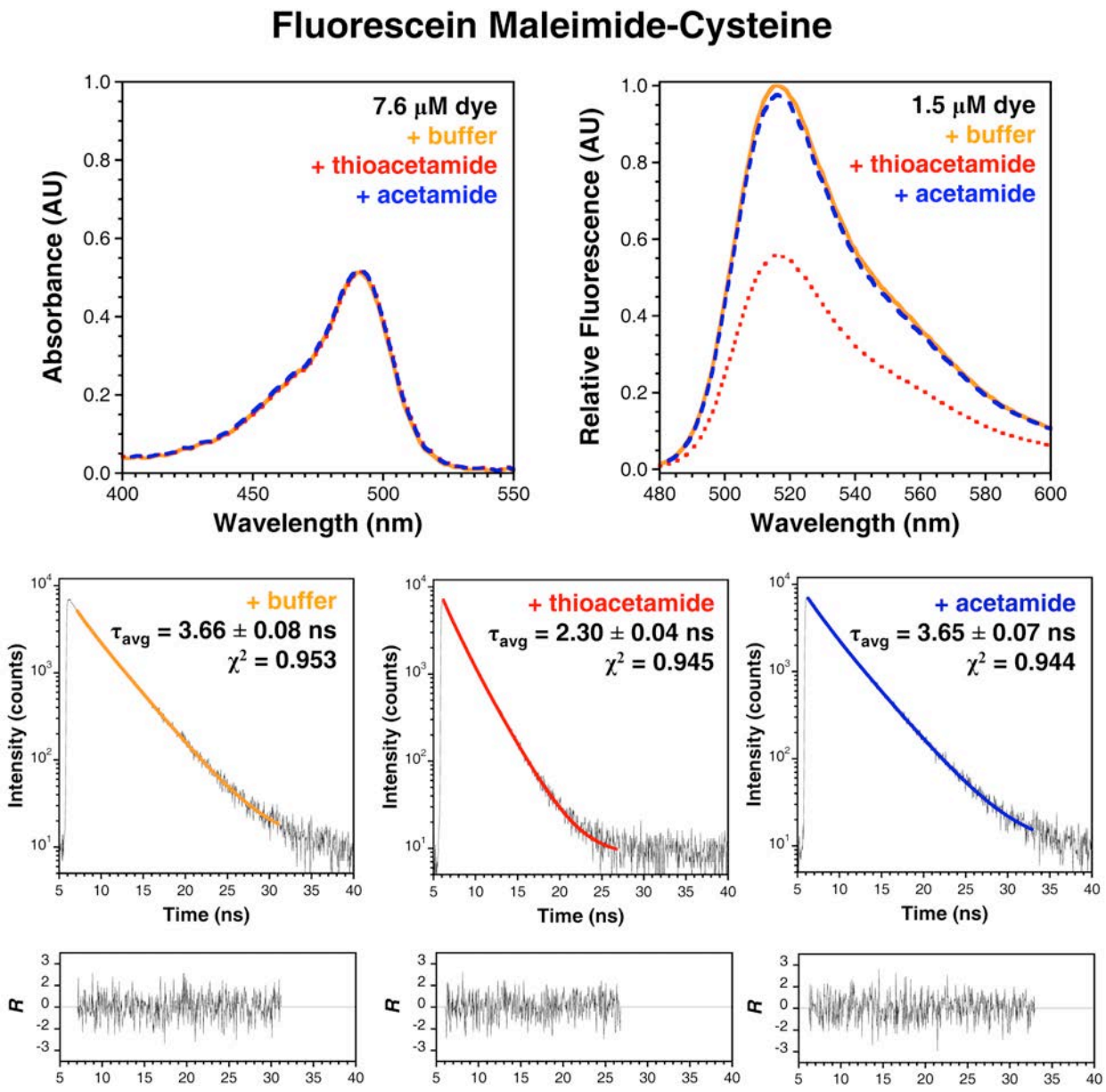

Figure S7. Fluorescein Maleimide-Cysteine (ψ, **17**). Background-corrected absorbance and normalized fluorescence (λ_{ex} = 450 nm) spectra of the fluorescein maleimide-cysteine conjugate (Fam-Cys, ψ, **17**) in 100 mM phosphate buffer, pH 7.00 (solid orange trace), 50 mM acetamide (dashed blue trace), and 50 mM thioacetamide (dotted red trace). Bi-exponential fits and weighted residuals of fluorescence lifetime measurements of the dye in buffer, 50 mM thioacetamide, and 50 mM acetamide. Reported lifetimes (τ_{avg}) are intensity-weighted averages of the long and short components. Concentration calculated from $\varepsilon_{494\ nm}$ = 68,000 M^{-1}•cm^{-1}.[5]

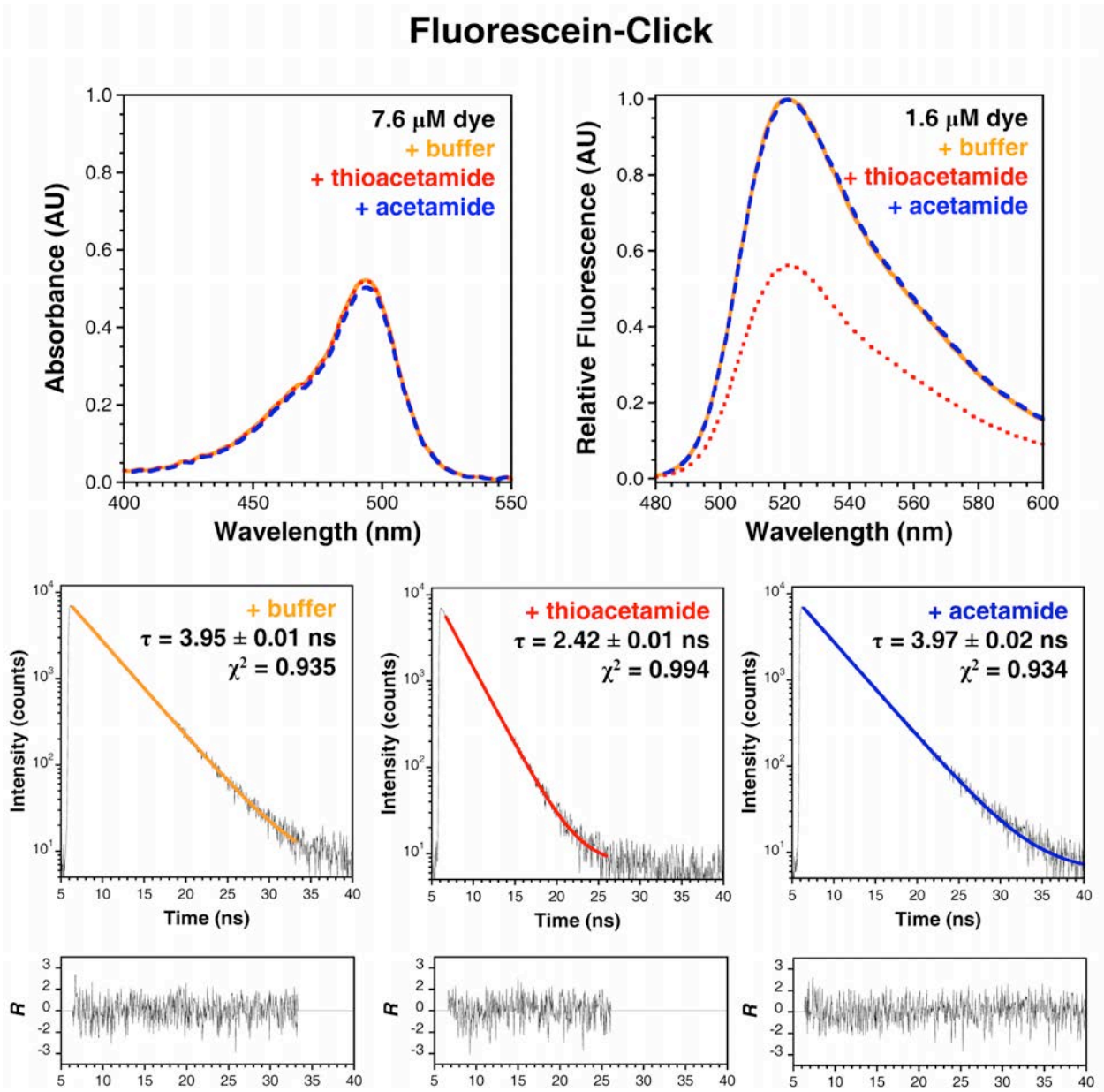

Figure S8. Fluorescein-Click (**15**). Background-corrected absorbance and normalized fluorescence (λ_{ex} = 450 nm) spectra of the Fam-Click conjugate (**15**) in 100 mM phosphate buffer, pH 7.00 (solid orange trace), 50 mM acetamide (dashed blue trace), and 50 mM thioacetamide (dotted red trace). Single-exponential fits and weighted residuals of fluorescence lifetime measurements of the dye in buffer, 50 mM thioacetamide, and 50 mM acetamide. Concentration calculated from $\varepsilon_{494\ nm}$ = 68,000 M^{-1}•cm^{-1}.[5]

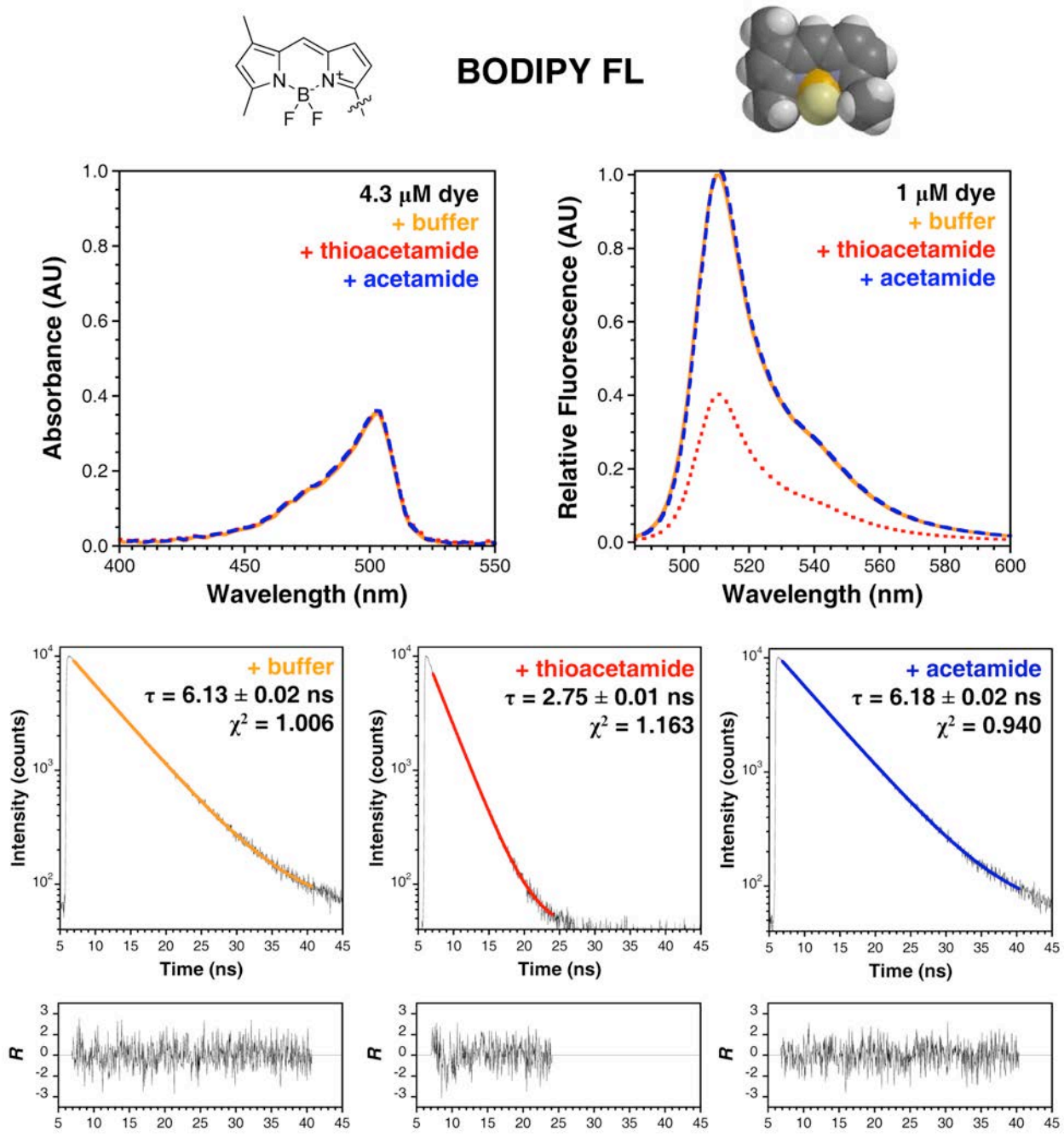

Figure S9. BODIPY FL (**10**). Chemical structure and space-filling model of BODIPY FL. Background-corrected absorbance and normalized fluorescence (λ_{ex} = 475 nm) spectra of the dye in 100 mM phosphate buffer, pH 7.00 (solid orange trace), 50 mM acetamide (dashed blue trace), and 50 mM thioacetamide (dotted red trace). Single-exponential fits and weighted residuals of fluorescence lifetime measurements of the dye in buffer, 50 mM thioacetamide, and 50 mM acetamide. Concentration calculated from $\varepsilon_{504\ nm}$ = 82,000 M^{-1}•cm^{-1}, the extinction coefficient provided by the manufacturer.[4]

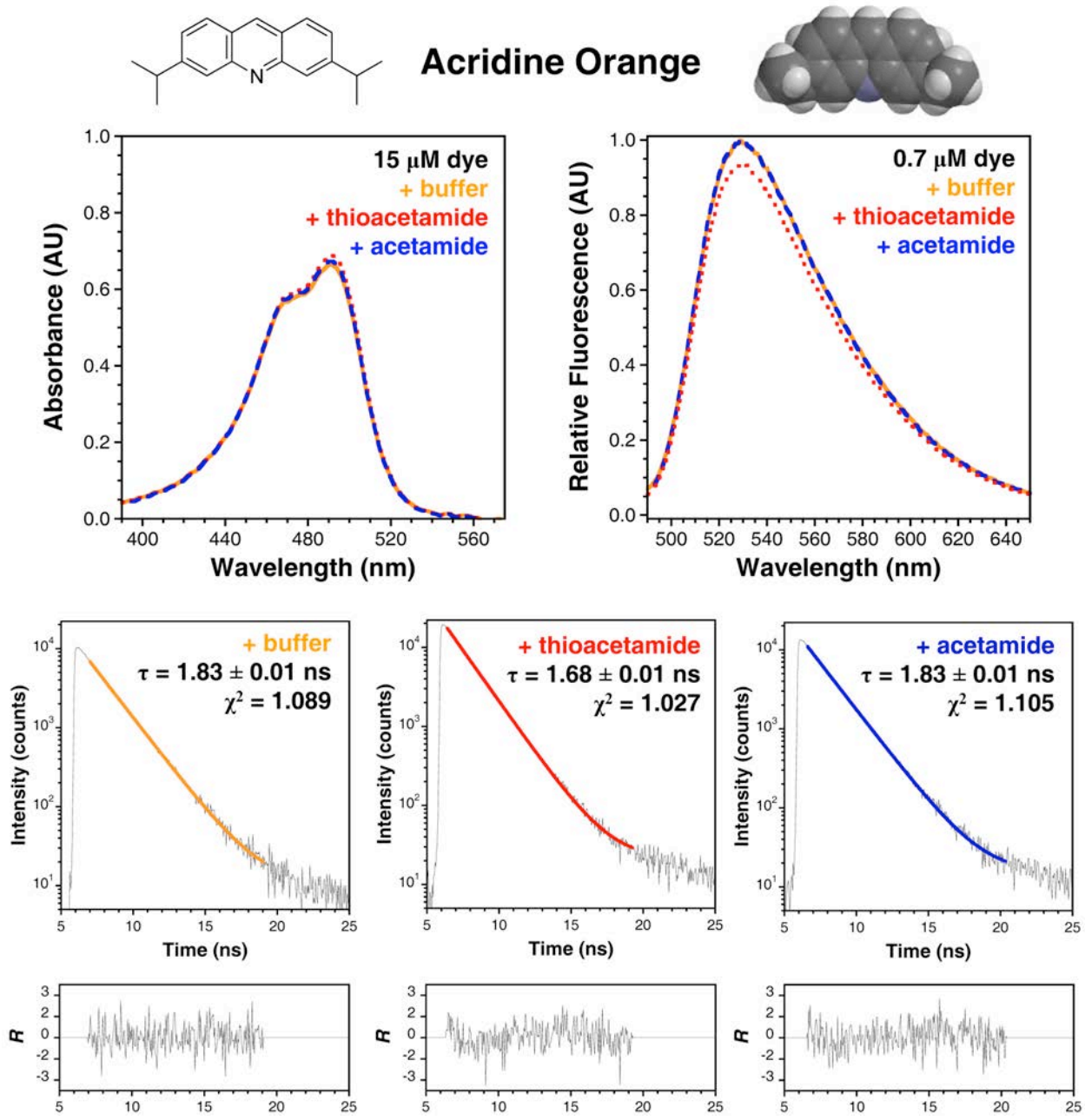

Figure S10. Acridine Orange (**3**). Chemical structure and space-filling model of acridine orange. Background-corrected absorbance and normalized fluorescence (λ_{ex} = 475 nm) spectra of the dye in 100 mM phosphate buffer, pH 7.00 (solid orange trace), 50 mM acetamide (dashed blue trace), and 50 mM thioacetamide (dotted red trace). Single-exponential fits and weighted residuals of fluorescence lifetime measurements of the dye in buffer, 50 mM thioacetamide, and 50 mM acetamide. Concentration calculated from $\varepsilon_{490\ nm}$ = 45,000 M^{-1}•cm^{-1}.[6]

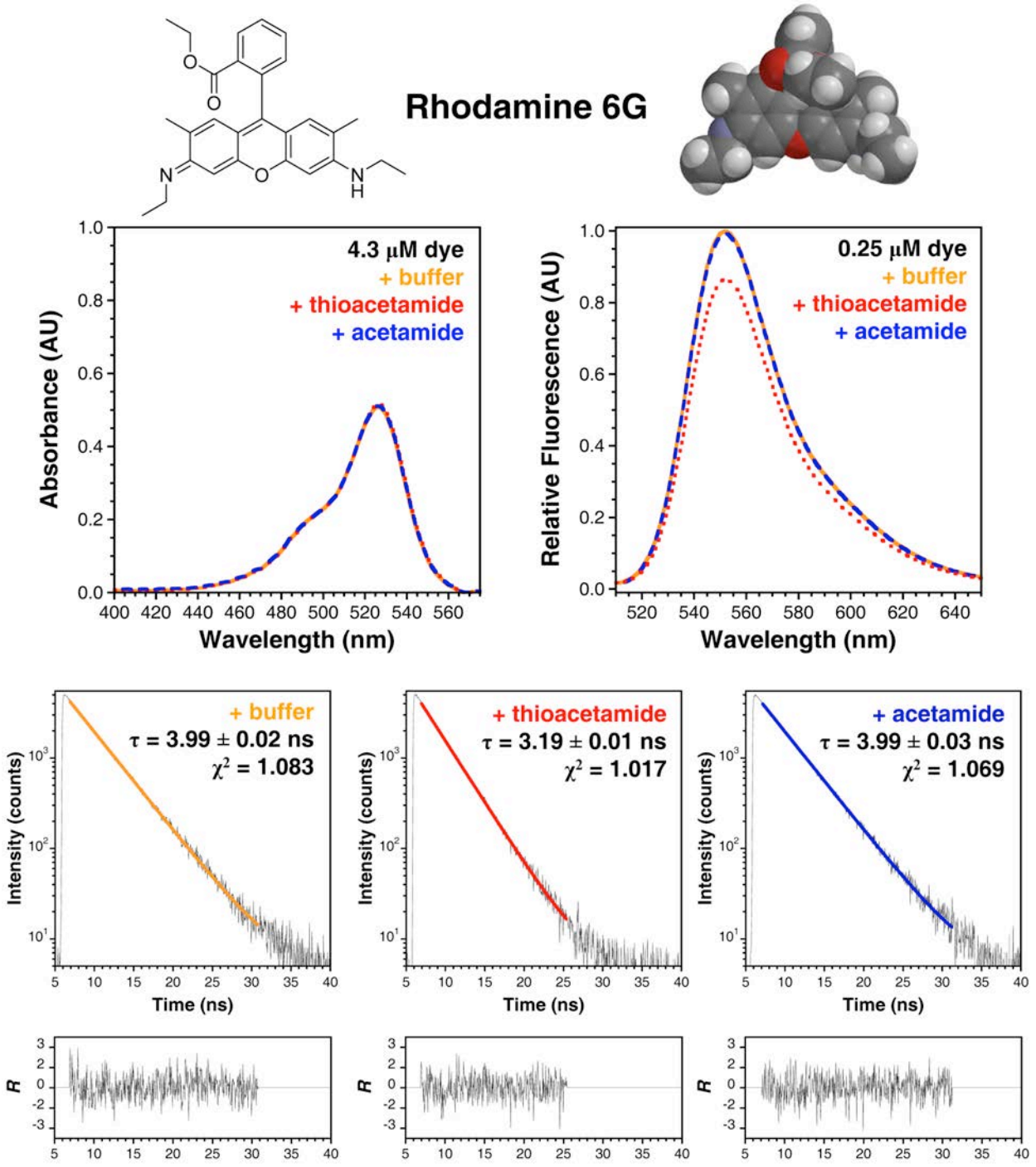

Figure S11. Rhodamine 6G (**13**). Chemical structure and space-filling model of rhodamine 6G. Background-corrected absorbance and normalized fluorescence (λ_{ex} = 500 nm) spectra of the dye in 100 mM phosphate buffer, pH 7.00 (solid orange trace), 50 mM acetamide (dashed blue trace), and 50 mM thioacetamide (dotted red trace). Single-exponential fits and weighted residuals of fluorescence lifetime measurements of the dye in buffer, 50 mM thioacetamide, and 50 mM acetamide. Concentration calculated from $\varepsilon_{528\ nm}$ = 116,000 M^{-1}•cm^{-1}.[7]

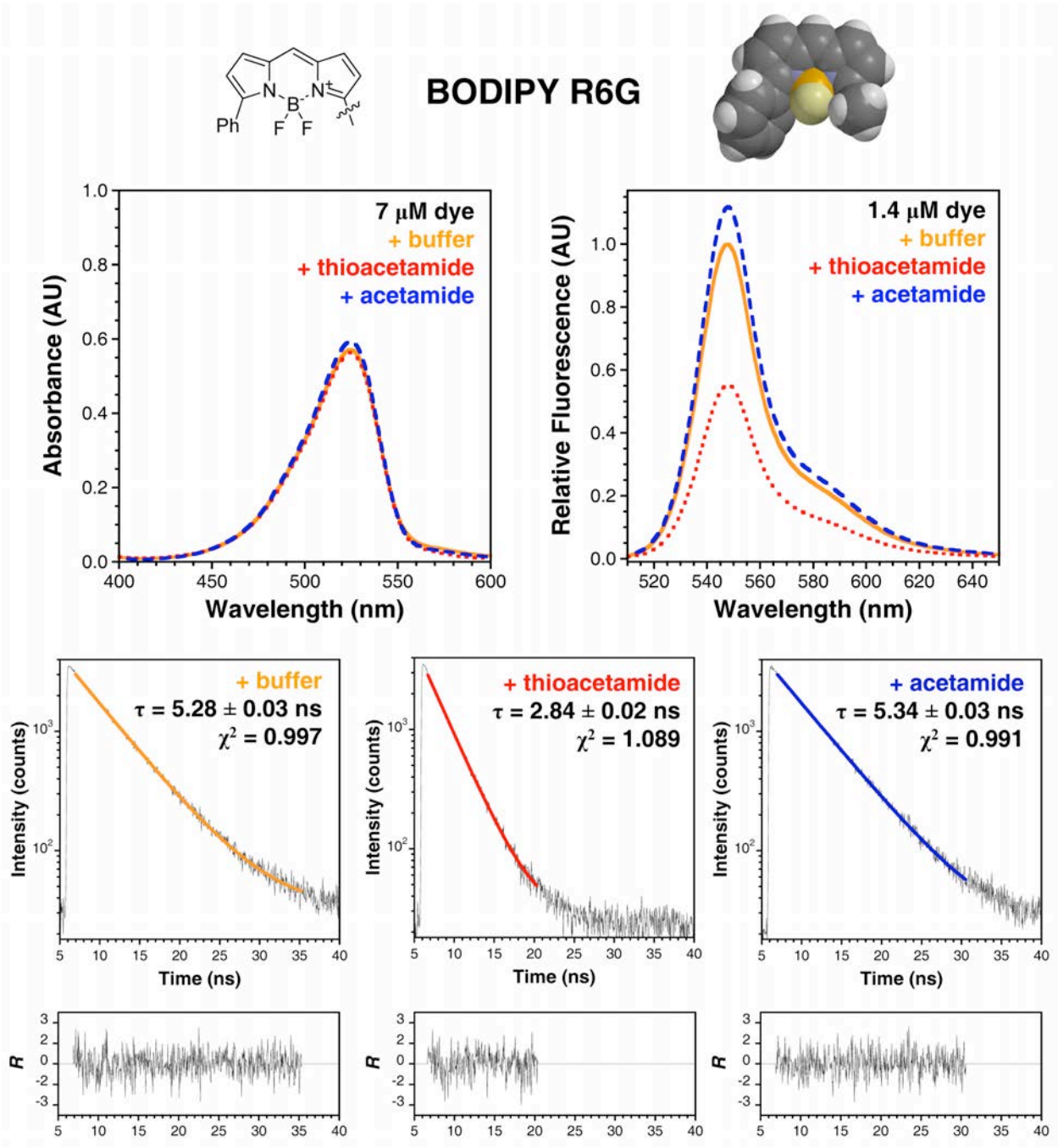

Figure S12. BODIPY R6G (**9**). Chemical structure and space-filling model of BODIPY R6G. Background-corrected absorbance and normalized fluorescence (λ_{ex} = 500 nm) spectra of the dye in 100 mM phosphate buffer, pH 7.00 (solid orange trace), 50 mM acetamide (dashed blue trace), and 50 mM thioacetamide (dotted red trace). Single-exponential fits and weighted residuals of fluorescence lifetime measurements of the dye in buffer, 50 mM thioacetamide, and 50 mM acetamide. All solutions contain 6.25% ethanol. Concentration calculated from $\varepsilon_{528\ nm}$ = 70,000 M^{-1}•cm^{-1}.[4]

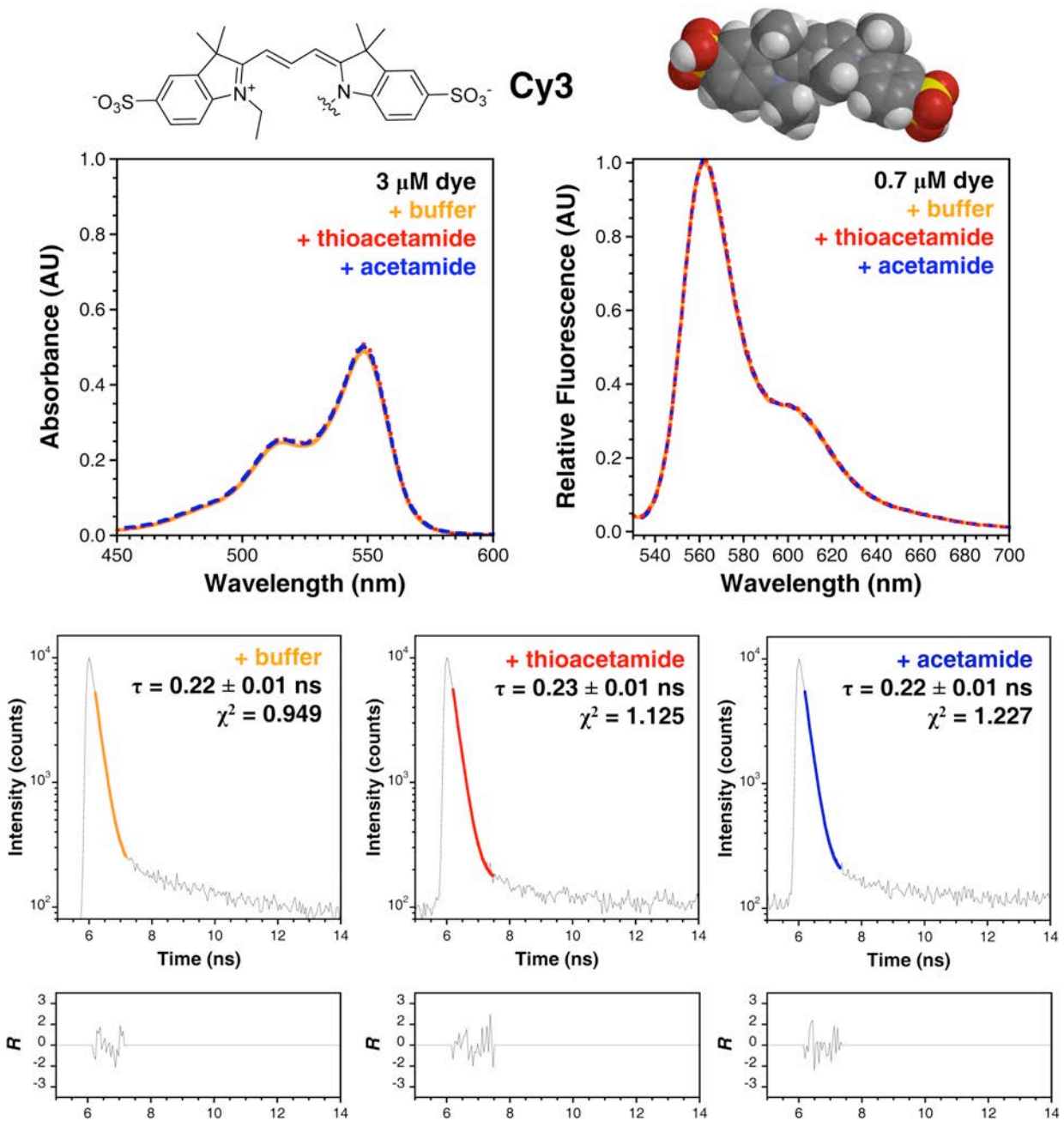

Figure S13. Cy3 (**7**). Chemical structure and space-filling model of Cy3. Background-corrected absorbance and normalized fluorescence (λ_{ex} = 520 nm) spectra of the dye in 100 mM phosphate buffer, pH 7.00 (solid orange trace), 50 mM acetamide (dashed blue trace), and 50 mM thioacetamide (dotted red trace). Single-exponential fits and weighted residuals of fluorescence lifetime measurements of the dye in buffer, 50 mM thioacetamide, and 50 mM acetamide. Concentration calculated from $\varepsilon_{550\ nm}$ = 150,000 M^{-1}•cm^{-1}.[8]

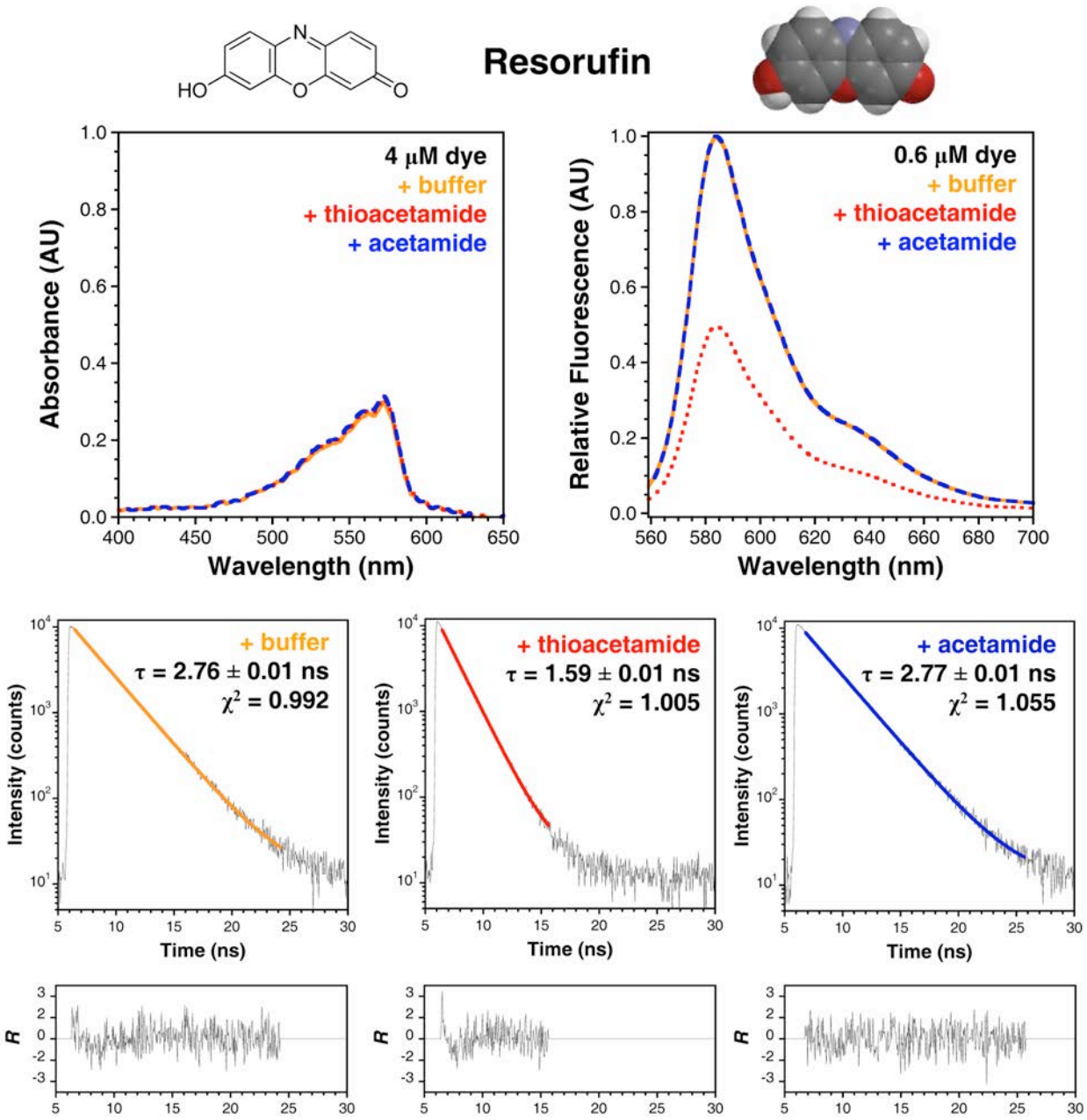

Figure S14. Resorufin (**5**). Chemical structure and space-filling model of resorufin. Background-corrected absorbance and normalized fluorescence (λ_{ex} = 550 nm) spectra of resorufin in 100 mM phosphate buffer, pH 7.00 (solid orange trace), 50 mM acetamide (dashed blue trace), and 50 mM thioacetamide (dotted red trace). Single-exponential fits and weighted residuals of fluorescence lifetime measurements of the dye in buffer, 50 mM thioacetamide, and 50 mM acetamide. Concentration calculated from $\varepsilon_{572\ nm}$ = 73,000 M^{-1}•cm^{-1}, the extinction coefficient provided by the manufacturer.

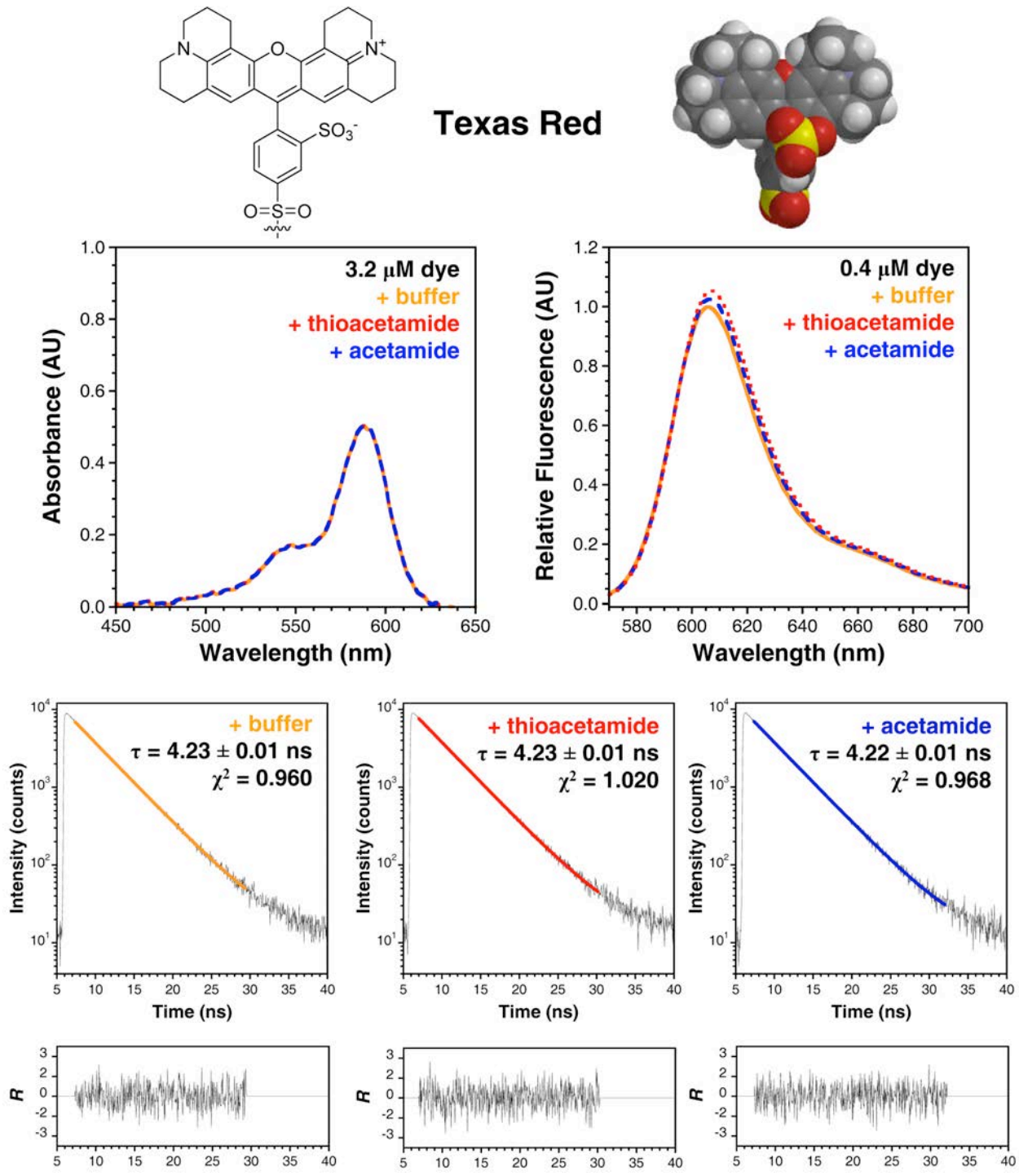

Figure S15. Texas Red (**11**). Chemical structure and space-filling model of Texas Red. Background-corrected absorbance and normalized fluorescence (λ_{ex} = 560 nm) spectra of the dye in 100 mM phosphate buffer, pH 7.00 (solid orange trace), 50 mM acetamide (dashed blue trace), and 50 mM thioacetamide (dotted red trace). Single-exponential fits and weighted residuals of fluorescence lifetime measurements of the dye in buffer, 50 mM thioacetamide, and 50 mM acetamide. Concentration calculated from $\varepsilon_{578\ nm}$ = 139,000 M^{-1}•cm^{-1}.[7]

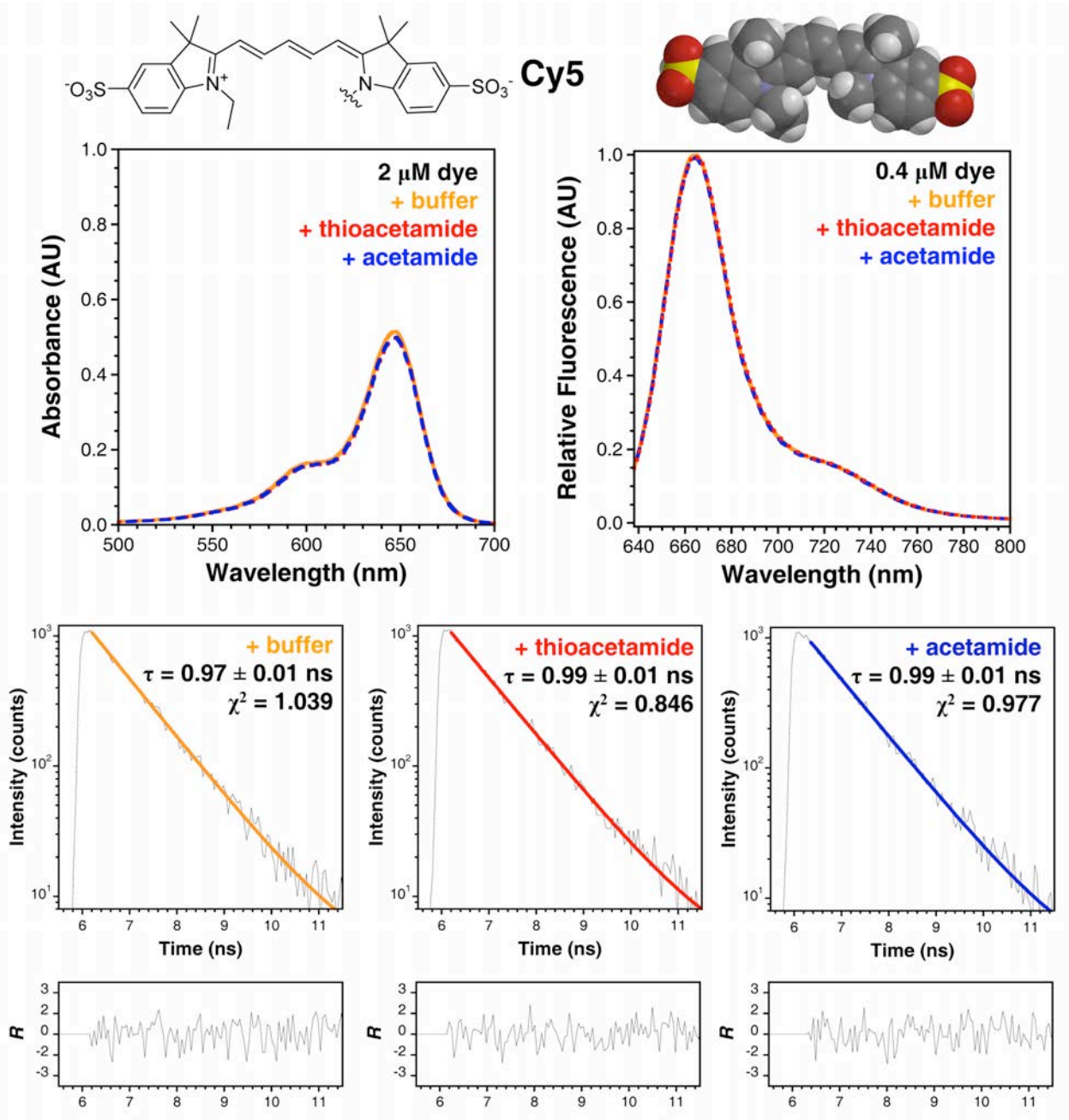

Figure S16. Cy5 (**8**). Chemical structure and space-filling model of Cy5. Background-corrected absorbance and normalized fluorescence (λ_{ex} = 630 nm) spectra of Cy5 in 100 mM phosphate buffer, pH 7.00 (solid orange trace), 50 mM acetamide (dashed blue trace), and 50 mM thioacetamide (dotted red trace). Single-exponential fits and weighted residuals of fluorescence lifetime measurements of the dye in buffer, 50 mM thioacetamide, and 50 mM acetamide. Concentration calculated from $\varepsilon_{650\ nm}$ = 250,000 M^{-1}•cm^{-1}.[8]

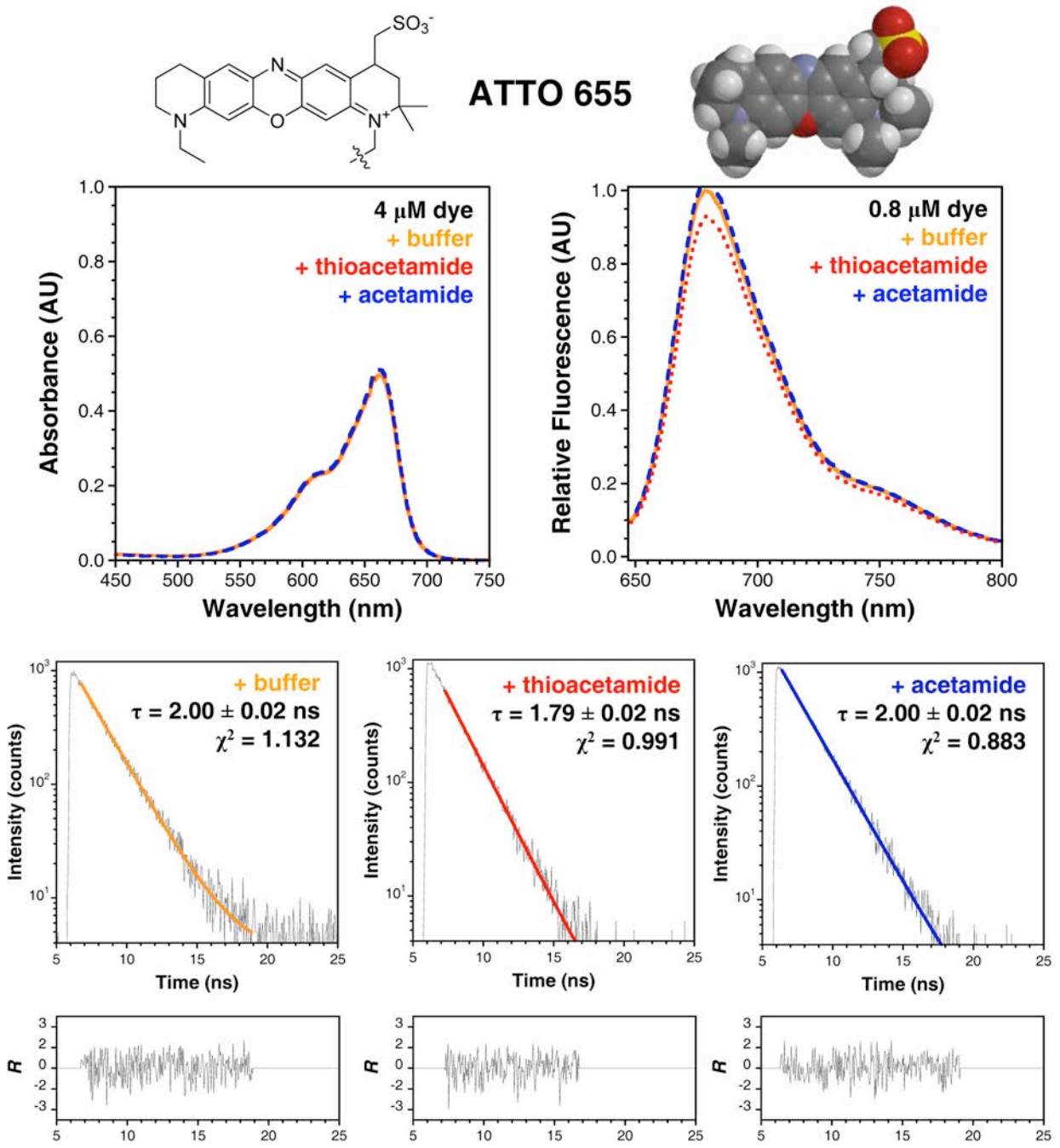

Figure S17. ATTO 655 (**6**). Chemical structure and space-filling model of ATTO 655. Background-corrected absorbance and normalized fluorescence (λ_{ex} = 640 nm) spectra of ATTO 655 in 100 mM phosphate buffer, pH 7.00 (solid orange trace), 50 mM acetamide (dashed blue trace), and 50 mM thioacetamide (dotted red trace). Single-exponential fits and weighted residuals of fluorescence lifetime measurements of the dye in buffer, 50 mM thioacetamide, and 50 mM acetamide. Concentration calculated from $\varepsilon_{663\ nm}$ = 120,000 M^{-1}•cm^{-1}, the extinction coefficient provided by the manufacturer.

Thiourea Quenching of 5-Carboxyfluorescein. The quenching efficiency of thiourea was determined by comparing the fluorescence of 5-carboxyfluorescein in the presence and absence of thiourea or urea. A concentrated stock of 5-carboxyfluorescein in 100 mM sodium phosphate buffer, pH 7.00 was used to prepare solutions that contained 1.6 μM fluorophore in pure buffer, 50 mM thiourea and buffer, or 50 mM urea and buffer. Fluorescence spectra of each sample were acquired in triplicate at 25 °C using the same parameters described above for the thioacetamide experiments (Fig. S18). The quenching efficiency, E_Q (SS) = 45 ± 1 %, was calculated using Equation S1 where F_0 was the fluorescence intensity at 520 nm in buffer and F was the fluorescence intensity at 520 nm of the 50 mM thiourea sample. The addition of urea or thiourea did not seem to change the absorbance spectrum of the dye (Fig. S18).

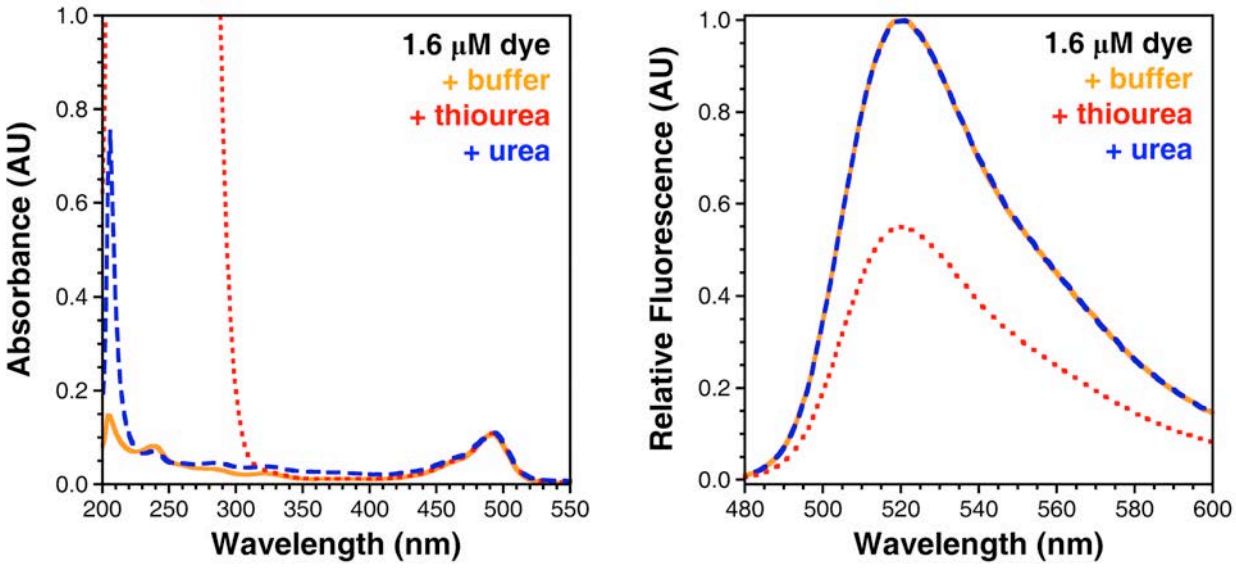

Figure S18. Thiourea Quenching of 5-Carboxyfluorescein. Background-corrected absorbance (left) and representative, normalized fluorescence (right, λ_{ex} = 450 nm) spectra of 1.6 μM 5-carboxyfluorescein in 100 mM phosphate buffer, pH 7.00 (solid orange trace), 50 mM urea (dashed blue trace), and 50 mM thiourea (dotted red trace).

Stern-Volmer Experiments. Concentrated stock solutions of 5-carboxyfluorescein or Alexa Fluor 488 in 100 mM sodium phosphate buffer, pH 7.00, were diluted with 100 mM thioacetamide and buffer to prepare samples of uniform dye concentration and variable thioacetemaide concentration (0, 2.5, 5, 15, 25, 35, 50, and 65 mM). The 5-carboxyfluorescein solutions were excited at 492 nm and emission was recorded from 500 to 600 nm (Fig. S19). The Alexa Fluor 488 solutions were excited at 475 nm and emission was recorded from 485 to 600 nm (Fig. S20). For all steady-state measurements, the excitation and emission slit widths were 5 nm, the scan rate was 120 nm/min, the data pitch was 1.0 nm, and the averaging time was 0.100 s. Measurements were made in 1.00 cm quartz cuvettes at 25 °C. For 5-carboxyfluorescein, the fluorescence intensity at 522 nm was averaged from three separate trials to obtain values for Stern-Volmer calculations. The fluorescence intensity at 516 nm from three separate trials was averaged to obtain values for Stern-Volmer calculations for the Alexa Fluor 488 samples.

The data sets for a given fluorophore were initially fit to a linear Stern-Volmer model (Eq. S6) with KaleidaGraph (Synergy Software; Reading, PA).

$$\frac{F_0}{F} = 1 + K_{SV}[Q] \qquad \text{(S6)}$$

Here, F_0 is the average fluorescence intensity at the wavelength of maximum fluorescence in the absence of quencher; F is the fluorescence intensity at the same wavelength at each thioacetamide concentration step; K_{SV} is the Stern-Volmer constant in M^{-1}; and [Q] is the molar concentration of the quencher (thioacetamide). The goodness-of-fit indicator R^2 was close to unity for both fluorophores ($R^2_{\text{5-carboxyfluorescein}} > 0.999$; $R^2_{\text{Alexa Fluor 488}} > 0.998$), and the linear fit described the 5-carboxyfluroescein data well. Despite the high coefficient of correlation, the linear model did not fit the Alexa Fluor 488 data satisfactorily. The values for K_{SV} obtained from

Equation S6 ($K_{SV,SS(5\text{-carboxyfluorescein})}$ = 15.13 ± 0.08 M^{-1}; $K_{SV,SS(Alexa\ Fluor\ 488)}$ = 16.94 ± 0.17 M^{-1}) were greater than those obtained under identical conditions from time-resolved measurements (Eq. S8, see below; $K_{SV,\tau(5\text{-carboxyfluorescein})}$ = 13.36 ± 0.04 M^{-1}; $K_{SV,\tau(Alexa\ Fluor\ 488)}$ = 14.75 ± 0.07 M^{-1}). This observation is consistent with a quenching mechanism that includes both static and dynamic components. Therefore, we chose to fit the steady-state Stern-Volmer data to Equation S7, which accounts for both static (K_S) and dynamic (K_D) quenching mechanisms (Fig. S19 – S20).

$$\frac{F_0}{F} = (1 + K_S[Q])(1 + K_D[Q]) \quad \text{(S7)}$$

In this analysis, we found roots of 13.68 ± 0.51 M^{-1} and 0.84 ± 0.31 M^{-1} for 5-carboxyfluorescein; and 13.42 ± 0.75 M^{-1} and 2.07 ± 0.48 M^{-1} for Alexa Fluor 488. Since the quenching appears to be dominated by a dynamic mechanism, we assigned the larger solution to K_D and the smaller solution to K_S. Thus, from the steady-state measurements, we found K_D = 13.68 ± 0.51 M^{-1} and K_S = 0.84 ± 0.31 M^{-1} for 5-carboxyfluorescein; and K_D = 13.42 ± 0.75 M^{-1} and K_S = 2.07 ± 0.48 M^{-1} for Alexa Fluor 488.

Time-resolved measurements were acquired on freshly prepared samples using the same experimental setup described above. The data sets were fit to a mono-exponential model (Eq. S2, n = 1) and the calculated lifetimes were used to construct linear Stern-Volmer plots using Equation S8 (Fig. S19 – S20).

$$\frac{\tau_0}{\tau} = 1 + K_{SV}[Q] \quad \text{(S8)}$$

In this equation, τ_0 is the fluorescence lifetime in the absence of quencher (4.04 ± 0.01 ns for 5-carboxyfluorescein and 4.03 ± 0.02 ns for Alexa Fluor 488); τ is the fluorescence lifetime at each thioacetamide concentration step; K_{SV} is the Stern-Volmer constant in units of M^{-1}; and [Q] is the molar concentration of the quencher (thioacetamide). We found $K_{SV,\tau}$ = 13.36 ± 0.04 M^{-1} for 5-carboxyfluorescein and $K_{SV,\tau}$ = 14.75 ± 0.07 M^{-1} for Alexa Fluor 488. These values are

comparable to those found for the dynamic quenching component in the steady-state experiments: For 5-carboxyfluorescein, K_D (13.68 ± 0.51 M^{-1}) and $K_{SV,\tau}$ (13.36 ± 0.04 M^{-1}) are the same within error. Quenching rate constants, k_Q = 3.31 ± 0.01 × 10^9 $M^{-1}s^{-1}$ for 5-carboxyfluorescein and k_Q = 3.66 ± 0.03 × 10^9 $M^{-1}s^{-1}$ for Alexa Fluor 488, were found using Equation S9.

$$K_{SV} = k_Q \tau_0 \quad \text{(S9)}$$

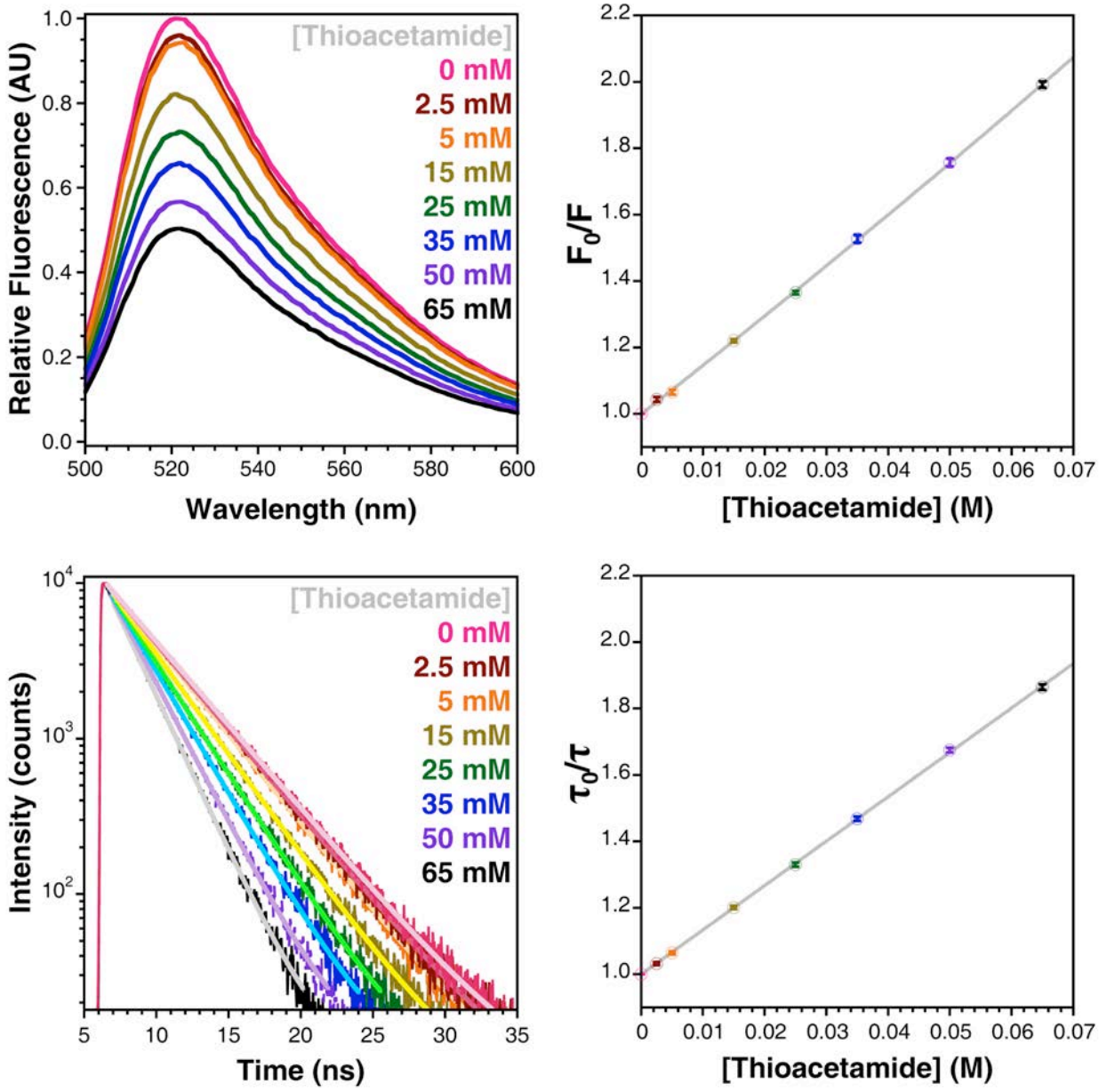

Figure S19. 5-Carboxyfluorescein Steady-State and Time-Resolved Stern-Volmer Experiments. Upper Left: 5-Carboxyfluorescein fluorescence with varying concentrations of thioacetamide in 100 mM sodium phosphate buffer, pH 7.00 at 25 °C (λ_{ex} = 492 nm). Upper Right: Stern-Volmer plot of thioacetamide quenching 5-carboxyfluorescein fit to Equation S7. Error bars are calculated from standard error. Lower Left: Normalized time-resolved fluorescence traces and mono-exponential fits of thioacetamide quenching 5-carboxyfluorescein (λ_{ex} = 405 nm; λ_{em} = 420 nm). Lower Right: Stern-Volmer plot of lifetime data fit to Equation S8. Error bars are estimated from fits; R^2 = 0.99988.

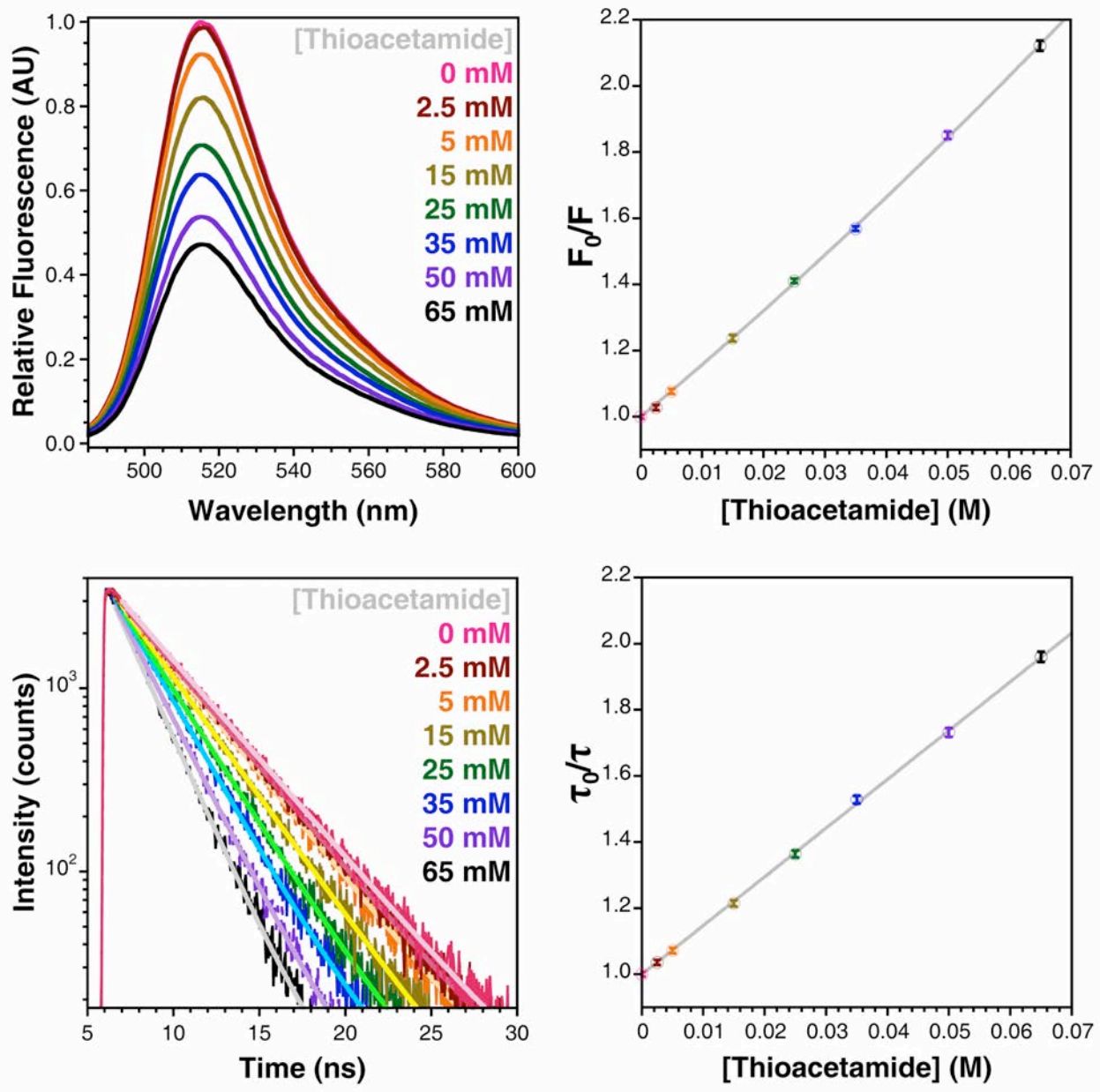

Figure S20. Alexa Fluor 488 Steady-State and Time-Resolved Stern-Volmer Experiments. Upper Left: Alexa Fluor 488 fluorescence with varying concentrations of thioacetamide in 100 mM sodium phosphate buffer, pH 7.00 at 25 °C (λ_{ex} = 492 nm). Upper Right: Stern-Volmer plot of thioacetamide quenching Alexa Fluor 488 fit to Equation S7. Error bars are calculated from standard error. Lower Left: Normalized, time-resolved fluorescence traces and mono-exponential fits of thioacetamide quenching Alexa Fluor 488 (λ_{ex} = 405 nm; λ_{em} = 520 nm). Lower Right: Stern-Volmer plot of lifetime data fit to Equation S8. Error bars are estimated from fits; R^2 = 0.99969.

Smoluchowski Equation Calculations. Theoretical values for the bimolecular collision quenching constant can be calculated by approximating the fluorophore and quencher to be hard spheres with radii R_A and R_B, respectively, colliding in solution with a rate constant given by Equation S10.

$$k_2 = \frac{2RT}{3\eta}\left(\frac{(R_A + R_B)^2}{R_A R_B}\right)(1000) \qquad \text{(S10)}$$

In this equation, R is the ideal gas constant (8.3145 kg•m^2•s^{-2}•K^{-1}•mol^{-1}), T is the temperature (in K) of the solution, η is the viscosity of the solvent, and 1000 is a conversion factor to relate L and m^3. A viscosity of 9.314×10^{-4} kg•m^{-1}•s^{-1} was used for 100 mM sodium phosphate solution at 298 K.[9] The radii of the fluorophore (R_A) and thioacetamide (R_B) were estimated from the equilibrium geometries calculated for each molecule using the AM1 semi-empirical method in Spartan (Fig. S21). The 5-carboxyfluorescein diameter (14.289 Å) was computed as the sum of the H4 to O7 distance, the van der Waals radius of hydrogen (1.200 Å), and the van der Waals radius of oxygen (1.520 Å).[10] The molecular van der Waals radius of 5-carboxyfluorescein (R_A = 7.145 Å) was taken to be half of this value. The diameter of Alexa Fluor 488 (15.408 Å) was computed as the sum of the O6 to O11 distance and twice the van der Waals radius of oxygen. The molecular van der Waals radius of Alexa Fluor 488 (R_A = 7.704 Å) was taken to be half of this value. For thioacetamide, the diameter (6.700 Å) was calculated as the sum of the S1 to H4 distance and the van der Waals radii of sulfur (1.851 Å) and hydrogen.[10] The molecular van der Waals radius of thioacetamide (3.350 Å) was computed as half of this value. Using these values, we calculated $k_2 = 8.2 \times 10^9$ M^{-1} s^{-1} for 5-carboxyfluorescein and $k_2 = 8.4 \times 10^9$ M^{-1} s^{-1} for Alexa Fluor 488. These values are of similar magnitude to the experimentally determined values $k_Q = 3.31 \pm 0.01 \times 10^9$ M^{-1}s^{-1} for 5-carboxyfluorescein and $k_Q = 3.66 \pm 0.03 \times 10^9$ M^{-1}s^{-1} for Alexa Fluor 488. The discrepancy between these values can be attributed to quenching efficiency

factors $f_Q = k_Q/k_2 = 0.40$ for 5-carboxyfluorescein and $f_Q = 0.40$ for Alexa Fluor 488 that account for the possibility that not all collisions result in quenching. It is also possible to attribute the differences between k_2 and k_Q to the coarseness of the approximations in the model.

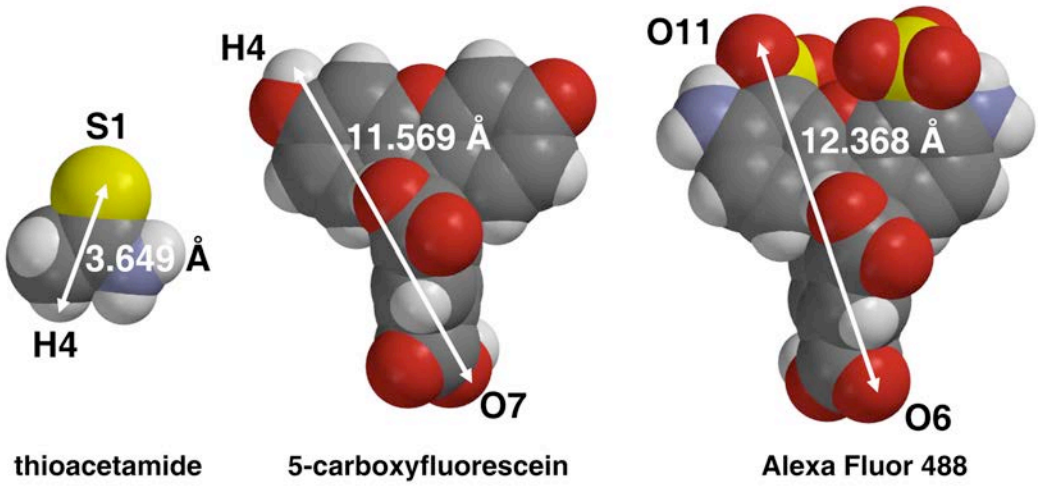

Figure S21. Equilibrium Geometries of Thioacetamide, 5-Carboxyfluorescein, and Alexa Fluor 488. Left: Thioacetamide S1 to H4 distance. Center: 5-Carboxyfluorescein H4 to O7 distance. Left: Alexa Fluor 488 O6 to O11 distance. Distances calculated in Spartan using the semi-empirical AM1 method.

Small Peptide Fluorescence Measurements. Fluorescence lifetime measurements were recorded for dilute (< 2 μM) solutions of the peptides $LP_2\psi$, $L'P_2\psi$, $LG_2\psi$, $L'G_2\psi$, $LP_3\psi$, $L'P_3\psi$, $LG_3\psi$, $L'G_3\psi$, AAFKGψ, and A'AFKGψ in 100 mM sodium phosphate buffer, pH 7.00 at 25 °C using the same parameters described above. The resulting data sets were fit to a single exponential function (Eq. S2; n = 1). We did not observe any reduction in lifetime of the thioamide P_2, G_2, or P_3 peptides relative to the corresponding oxo-amide peptides. We saw a small amount of quenching in the G_3 peptides (6.0 ± 0.4 %) and a modest amount of quenching in the AAFKGψ peptides (18.5 ± 0.5 %) as shown in Figure S22.

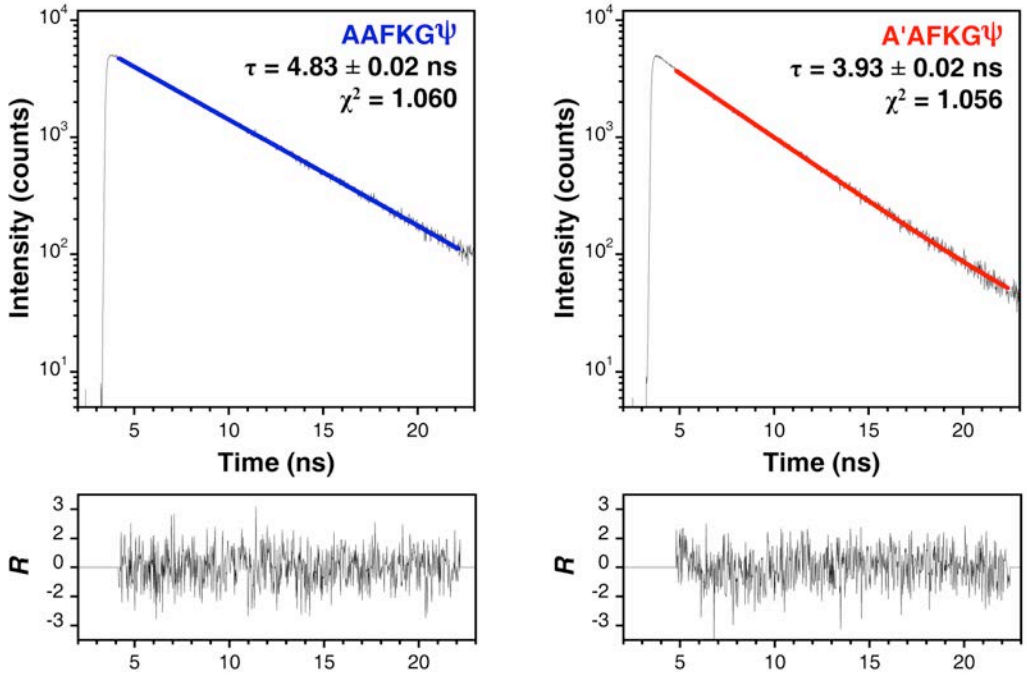

Figure S22. Fluorescence Lifetime Measurements of Fluorescein Labelled Peptides. Single-exponential fits and weighted residuals of fluorescence lifetime measurements of AAFKGψ and A'AFKGψ as indicated.

Monte Carlo Simulations. Monte Carlo simulations were used to estimate the ground state conformer distribution of L'P$_2$ψ, L'G$_2$ψ, L'P$_3$ψ, and L'G$_3$ψ. The structure of each peptide was modeled in Spartan (Wavefunction, Inc.; Irvine, CA) and a Monte Carlo algorithm allowing for rotatable bonds and a normal rule set was used with the aqueous Merck Molecular Force Field (MMFF aq) to examine 10,000 conformers. The 100 lowest-energy conformers from these simulations were kept for further analysis. The distance between the C=S carbon atom (C1) of the thioamide and various atoms of the fluorescein xanthene ring (designated C2, C3, and O1) were calculated for each structure. The mean values and standard deviations for each measurement are reported in Figures S23 – S24. Models representative of compact and extended conformations are shown in Figures S23 – S24. Histograms showing the distribution of the C1 – C2 distances are presented in Figure S25. We note that more instances of close approach R(C1 – C2) < 5.5 Å are seen for L'G$_3$C-Fam than for the other peptides. If van der Waals contact is necessary for thioamide quenching of fluorescein, an increase in the frequency of these transient interactions would explain why quenching is observed only for the L'G$_3$ψ peptide.

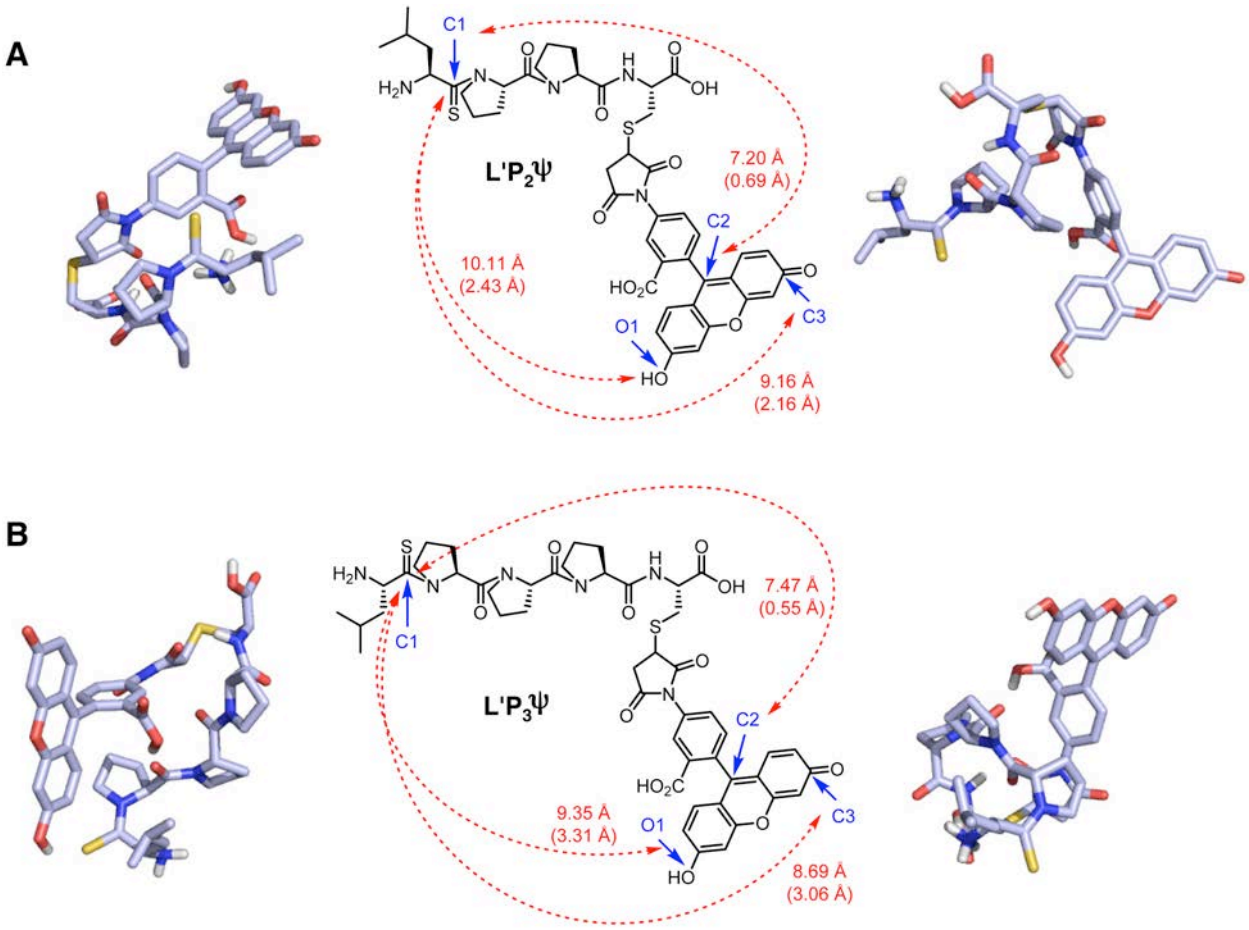

Figure S23. Conformational Analysis of Proline Peptides. Average distances and standard deviations between C1 and C2, C1 and C3, and C1 and O1 in L'P_2ψ (A) and L'P_3ψ (B) peptide ensembles generated from Monte Carlo simulations as described in the text. Models of representative compact (left) and extended (right) conformations rendered in PyMOL (Schrödinger; Portland, OR).

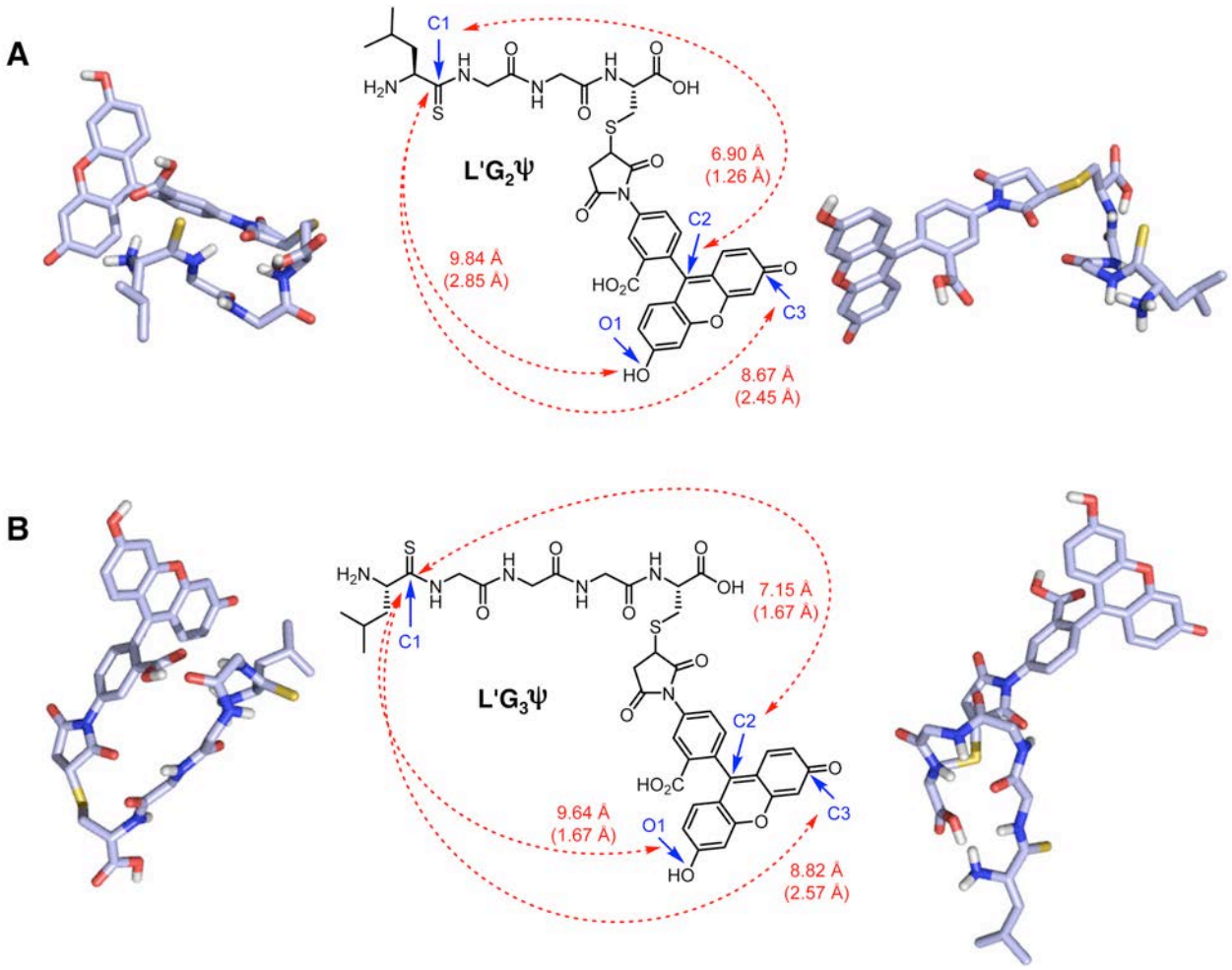

Figure S24. Conformational Analysis of Glycine Peptides. Average distances and standard deviations between C1 and C2, C1 and C3, and C1 and O1 in L'G_2ψ (A) and L'G_3ψ (B) peptide ensembles generated from Monte Carlo simulations as described in the text. Models of representative compact (left) and extended (right) conformations rendered in PyMOL (Schrödinger; Portland, OR).

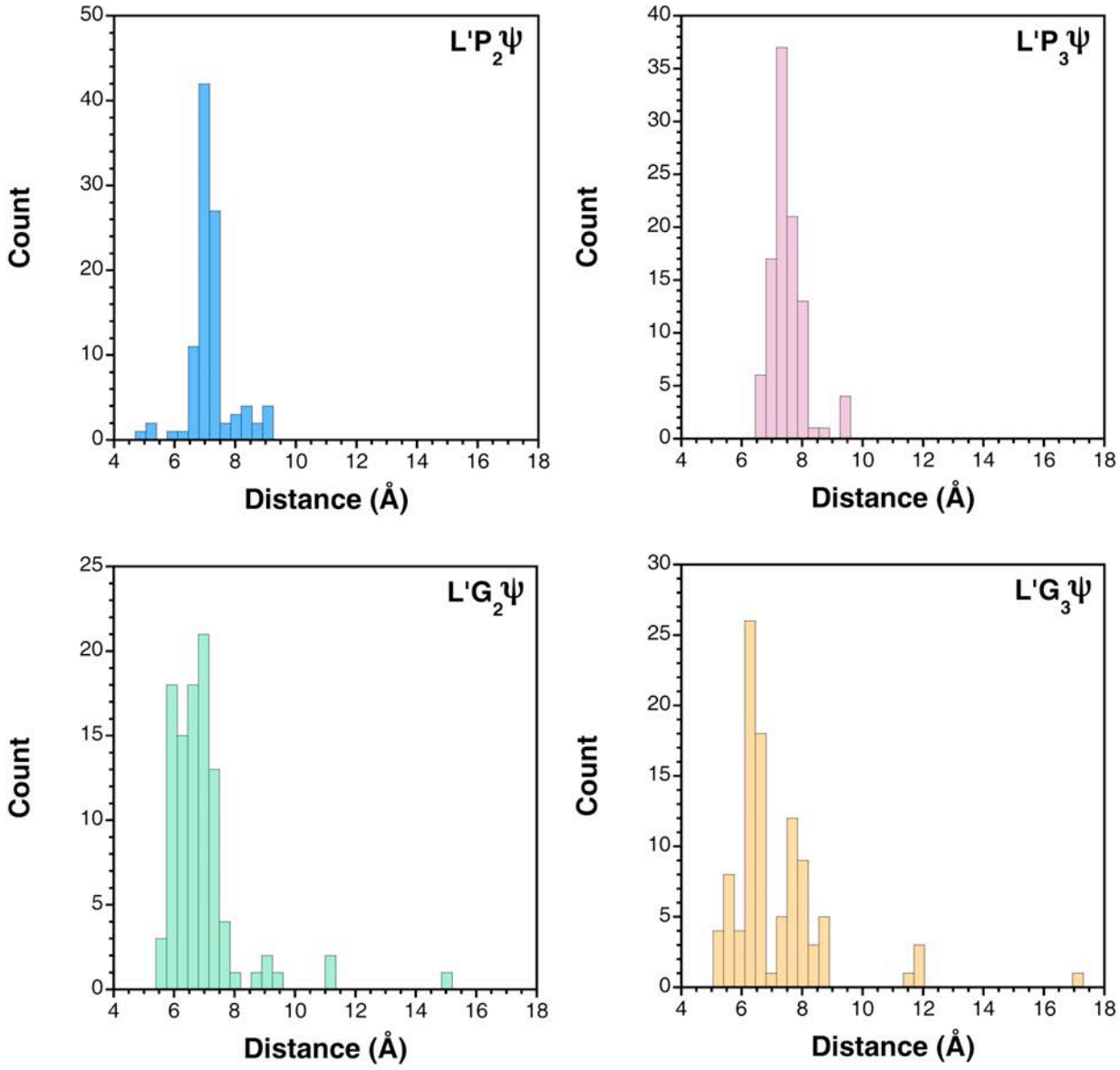

Figure S25. Distribution of C1 – C2 Distances in Proline and Glycine Peptides. Histograms showing the distribution of C1 – C2 distances in the conformer ensembles generated from Monte Carlo simulations.

Protease Experiments. A sample of trypsin type II from porcine pancreas (Sigma-Aldrich; 1,000-2,000 units/mg) was dissolved in cold 1 mM hydrochloric acid at a concentration of 2.5 mg/mL. Concentrated stocks of AAFKGψ and A'AFKGψ peptides in 67 mM sodium phosphate buffer, pH 7.6 were prepared and cooled on ice. Samples (1 mL total volume) were prepared in triplicate immediately before fluorescence measurements were taken such that the final concentration of peptide was approximately 1.4 μM and the final concentration of trypsin was 250 μg/mL. Samples of equimolar peptide in an equivalent HCl/buffer solution in the absence of enzyme were used as controls. The fluorescence of each sample was measured over the course of 45 min with the kinetics module of a Varian Cary Eclipse fluorescence spectrophotometer fitted with a Peltier multicell holder. The excitation wavelength was 494 nm and the emission wavelength was 522 nm. The excitation and emission slit widths were both 5 nm. The averaging time was 0.100 s. The fluorescence of each sample of was measured at 20 °C using quartz fluorometer cells with path lengths of 1.00 cm with magnetic stirring. The average fluorescence from each of three independent trials of the thiopeptide in the presence and absence of enzyme are shown in the main text (Fig. 3) with the standard error. Representative traces from the AAFKGψ peptides in the presence and absence of trypsin are shown in Figure S26.

Previous Trypsin Experiments. We have collected k_{cat} and K_M data from several previous investigations of trypsin proteolysis. These experiments were performed with short peptide substrates similar to our own, with a canonical Lys or Arg site for trypsin proteolysis. Initial rates (v_0) were calculated using Equation S11 for an experiment with an initial concentration of 1.4 μM substrate ($[S]_0$) and 0.05 μM active trypsin ($[E]_0$), corresponding to 0.5% of a 10 μM total loading, typical of commercial grade trypsin.[11]

$$v_0 = \frac{k_{cat}[\mathrm{E}]_0[\mathrm{S}]_0}{[\mathrm{S}]_0 + K_M} \qquad \text{(S11)}$$

As one can see, there is a very large range among these initial rates.

Table S2. Previous Measurements of Trypsin Kinetics with Peptide Substrates.

Peptide	k_{cat} (min^{-1})	K_M (μM)	v_0 (μM•min^{-1})
LysNA[a]	0.18	364	3.5×10^{-5}
CbzArgTl[b]	41.4	1400	2.07×10^{-3}
BzArgNA[c]	87	93	6.5×10^{-2}
BzValGlyArgNA[d]	26400	167	11.0
TsGlyMetLysAMC[e]	3155	14	14
TsGlyProArgAMC[f]	4450	4.8	50

a. Lysine *p*-nitroanilide,[12] b. *N*-Benzyloxycarbonyl arginine *p*-toluidide,[13] c. *N*-Benzoyl arginine *p*-nitroanilide,[14] d. *N*-Benzoyl valylglycylarginine *p*-nitroanilide,[14] e. *N*-Tosyl glycylmethionyllysine,[11] f. *N*-Tosyl glycylprolylarginine[11]

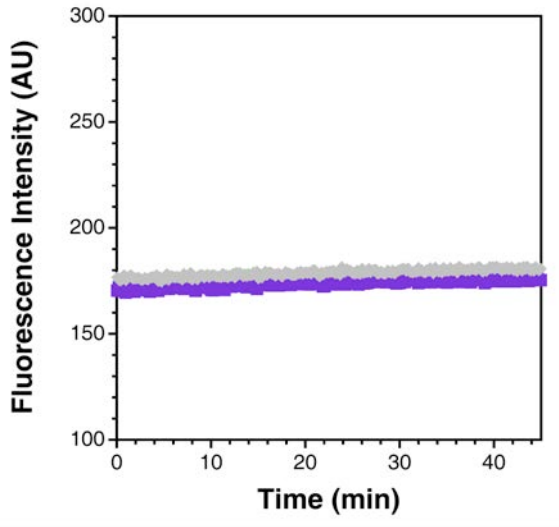

Figure S26. Protease Activity Monitored with Oxo-amide Peptides. Fluorescence of 1.4 μM AAFKGψ in the presence (gray diamonds) and absence (purple squares) of 250 μg/mL trypsin in 67 mM sodium phosphate buffer, pH 7.6. Excitation was at 494 nm and emission was monitored at 522 nm.

Synthesis of $\alpha S_{114\text{-}140}C_{114}E'_{137}$ and $\alpha S_{125\text{-}140}C_{125}E'_{130}$.

Scheme S1. Thioglutamate Precursor (**S5**). *N*-Methyl morpholine (NMM), isobutyl chloroformate (IBCF)

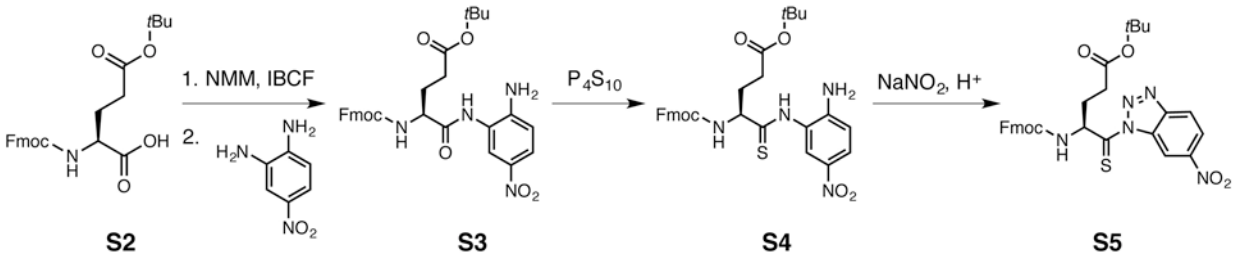

The synthesis of Fmoc-L-thioglutamate(O*t*Bu)-nitrobenzotriazolide precursor (**S5**) was based on a minor modification of the procedure originally reported by Shalaby *et al.*[15,16]

C-terminal peptides $\alpha S_{114\text{-}140}C_{114}E'_{137}$ (CDMPVDPDNEAYEMPSEEGYQDYE'PEA) and $\alpha S_{125\text{-}140}C_{125}E'_{130}$ (CEMPSE'EGYQDYEPEA) were synthesized on the 100 μmol scale on 2-chlorotrityl resin using a manual, Fmoc-based solid phase procedure as described above with the following modifications. For both peptides, a double coupling and a single Fmoc-deprotection were employed for all natural amino acids. Fmoc-L-thioglutamate(O*t*Bu)-nitrobenzotriazole (**S5**) was used to install thioglutumate at position 130 or 137. For the coupling of thioglutamate, using the coupling of E'_{130} for $\alpha S_{125\text{-}140}C_{125}E'_{130}$ as an example, dry CH_2Cl_2 was used as a solvent in order to avoid a water-dependent side reaction resulting in misincorporation of glutamate in place of thioglutatmate. After Fmoc deprotection of E_{131} in DMF, the resin beads were washed thoroughly with DMF followed by with dry CH_2Cl_2. The thioglutamate precursor (5 equiv; 145 mg) was dissolved in 4 mL dry CH_2Cl_2 in a vial. The solution was vortexed and added to the RV. The vial was rinsed with 2 mL dry CH_2Cl_2, and the solution was added to the RV. Then, DIPEA (10 equiv; 175 μL) was added to the RV (it is important not to add DIPEA to the benzotriazole solution as this can degrade the benzotriazole). The coupling reaction was carried out twice for 90 min. After each coupling, the spent solution was removed with vacuum suction

and the resin beads were washed thoroughly with dry CH_2Cl_2. Fmoc deprotection of E'_{130} and the rest of the peptide elongation were carried out in DMF, following the standard SPPS procedure. Each peptide was cleaved with 10 mL of a freshly made cleavage cocktail of 18:1:1 (v/v) TFA/CH_2Cl_2/TIPS for 1.5 h at RT. The cleavage solution was concentrated by rotary evaporation and the peptide was precipitated by the addition of a 10-fold excess of cold diethyl ether.

Both peptides were purified to homogeneity by reverse-phase HPLC on a Vydac 218TP C18 semi-prep column using a linear solvent gradient consisting of an aqueous phase (H_2O + 0.1% CF_3CO_2H) and organic phase (CH_3CN + 0.1% CF_3CO_2H). For $\alpha S_{114\text{-}140}C_{114}E'_{137}$, the gradient was isocratic at 98% aqueous phase for 5 min and then ranged from 98% to 81% aqueous phase over 5 min, then to 77% aqueous phase over 18 min, then to 0% aqueous phase over 2 min, remained at 0% for 5 min, then returned to 98% aqueous phase during a 5 min wash out period. The retention time of $\alpha S_{114\text{-}140}C_{114}E'_{137}$ was 25.8 min using this gradient. For $\alpha S_{125\text{-}140}C_{125}E'_{130}$, the gradient was isocratic at 98% aqueous phase for 5 min and then ranged from 98% to 85% aqueous phase over 5 min, then to 80% aqueous phase over 18 min, then to 0% aqueous phase over 2 min, remained at 0% for 5 min, then returned to 98% aqueous phase during a 5 min wash out period. The retention time of $\alpha S_{125\text{-}140}C_{125}E'_{130}$ was 25.4 min using this gradient. MALDI MS m/z calcd for $\alpha S_{114\text{-}140}C_{114}E'_{137}$ $(M\text{-}H)^-$ 3137.16, found 3137.28. MALDI MS m/z calcd for $\alpha S_{125\text{-}140}C_{125}E'_{130}$ $(M\text{-}H)^-$ 1890.62, found 1890.52. Purified peptides were dried in a vacuum centrifuge.

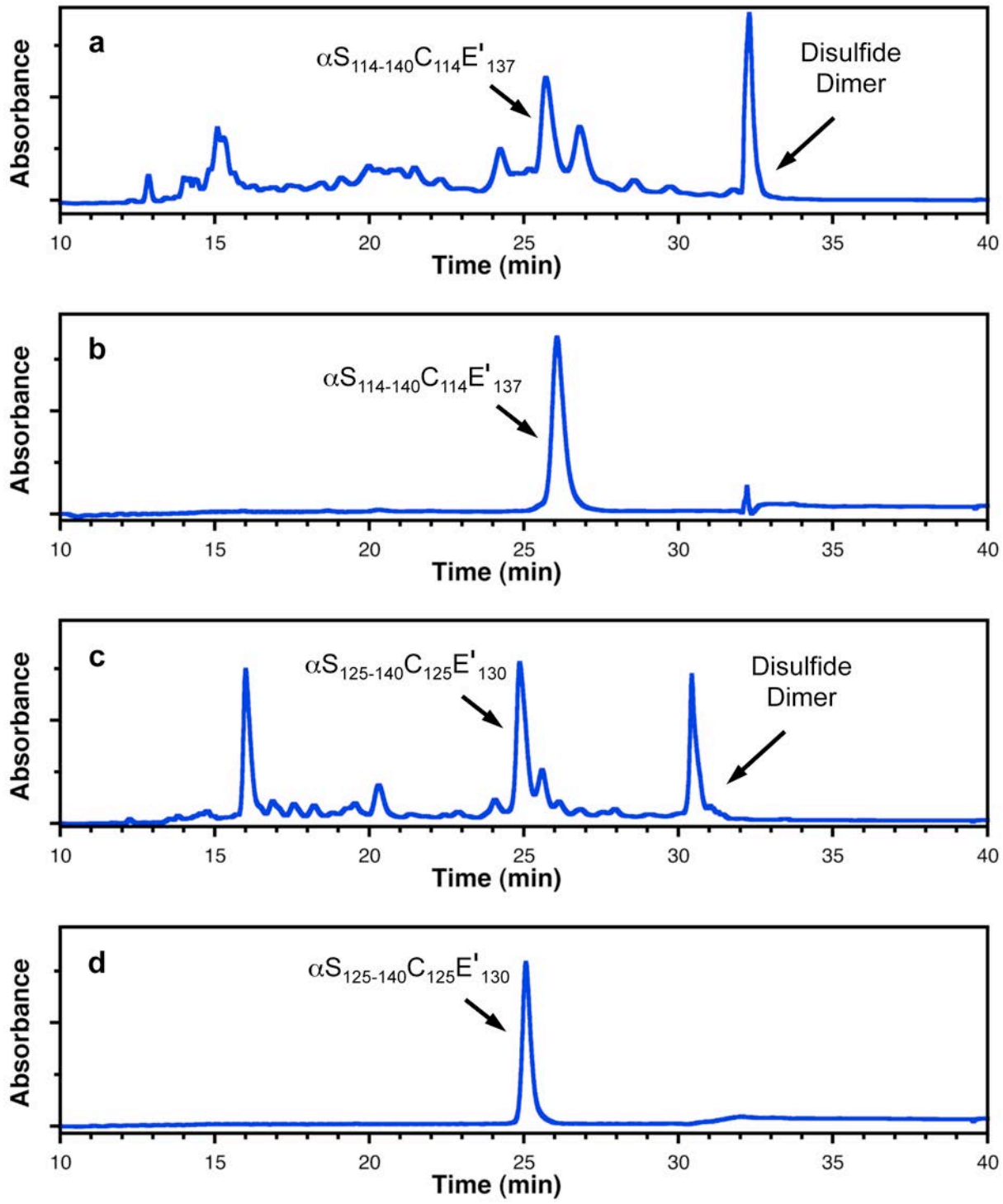

Figure S27. HPLC Chromatograms of $\alpha S_{114\text{-}140}C_{114}E'_{137}$ and $\alpha S_{125\text{-}140}C_{125}E'_{130}$. (a) Crude $\alpha S_{114\text{-}140}C_{114}E'_{137}$, (b) Purified $\alpha S_{114\text{-}140}C_{114}E'_{137}$, (c) Crude $\alpha S_{125\text{-}140}C_{125}E'_{130}$, (d) Purified $\alpha S_{125\text{-}140}C_{125}E'_{130}$; UV absorbance monitored at 271 nm. Peak assignments based on MALDI MS analysis.

Construction of pRK αS Cys Mutant Expression Plasmid (Oxoamide Control Protein). A plasmid containing the human wild-type αS gene cloned between NdeI and HindIII in the expression vector pRK172 was provided by Dr. Virginia Lee (Perelman School of Medicine, University of Pennsylvania). QuikChange® mutagenesis was used to mutate Glu_{114} to Cys_{114} and Tyr_{125} to Cys_{125} in the pRK172 construct to yield pRK172-αSC_{114} and pRK172-αSC_{125}, respectively. The sequence of the mutant plasmid was confirmed by DNA sequencing analysis. DNA primers for each mutagenesis step are shown in Figure S29.

Construction of pTXB1 αS Npu-His_6 Expression Plasmid. The ubiquitin-intein pTXB1-Ub-NpuDnaE-AAFN-His_6 plasmid was provided by Dr. Tom Muir (Princeton University).[17] The first six nucleotides of the NpuDnaE intein (TGTTTA) were mutated to TGCCTG using QuikChange® mutagenesis. A PacI site (TTAATTAA) was introduced at Gly_{76} of ubiquitin (Ub) and Cys_1 of Npu (GGTTGC) using QuikChange® mutagenesis (Fig. S28d). The resulting plasmid was digested with NdeI and PacI, then gel purified to remove the Ub gene.

A plasmid containing the human wild-type $\alpha S_{1\text{-}122}$ gene immediately followed by MxeGyrA-His_6 in pTXB1 vector (pTXB1-$\alpha S_{1\text{-}122}$-MxeGyrA-His_6) was modified to replace the MxeGyrA intein with the NpuDnaE intein (the generation of pTXB1-$\alpha S_{1\text{-}122}$-MxeGyrA-His_6 has been described previously).[18] A PacI site (TTAATTAA) was introduced between N_{122} of αS and C_1 of MxeGyrA using QuikChange® mutagenesis (Fig. S28b). The $\alpha S_{1\text{-}122}$ gene was digested by NdeI and PacI, gel purified, and ligated into the NdeI/PacI site of the pTXB1 vector containing NpuDnaE-His_6 to generate pTXB1-$\alpha S_{1\text{-}122}$-PacI-NpuDnaE-His_6 (Fig. S28e). QuikChange® mutagenesis was used to sequentially delete the PacI site and then the base pairs corresponding to residues $\alpha S_{114\text{-}122}$ to obtain pTXB1-$\alpha S_{1\text{-}113}$NpuDnaE-His_6 (Fig. S28f). Separately, pTXB1-$\alpha S_{1\text{-}122}$-PacI-NpuDnaE-His_6 was treated with primers that inserted base pairs corresponding to

residues E_{123} and A_{124} while simultaneously deleting the PacI site to generate pTXB1-αS_{1-124}NpuDnaE-His_6 (Fig S28g). DNA primers for each mutagenesis step are shown in Figure S29. The mutations were verified by DNA sequencing with a T7 promoter primer.

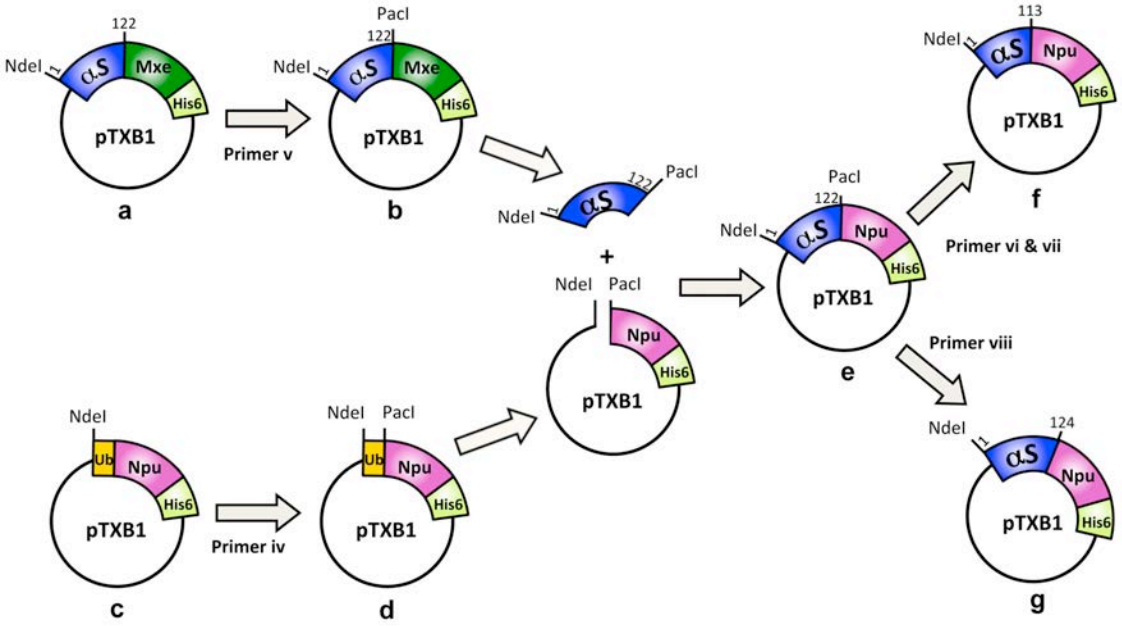

a. – CCT GAC AAT TGC ATC –
P_{120} D_{121} N_{122} C_1 I_2

PacI

b. – CCT GAC AA TTAATTAA GC ATC –
P_{120} D_{121} N_{122} C_1 I_2

c. – AGA GGT GGT TGC CTG AGC –
R_{74} G_{75} G_{76} C_1 L_2 S_3

PacI

d. – AGA GGT GG TTAATTAA GC CTG AGC –
R_{74} G_{75} G_{76} C_1 L_2 S_3

PacI

e. – CCT GAC AA TTAATTAA GC CTG AGC –
P_{120} D_{121} N_{122} C_1 L_2 S_3

g. – CCT GAC AAT GAG GCT TGC CTG AGC –
P_{120} D_{121} N_{122} E_{123} A_{124} C_1 L_2 S_3

f. – CAG GAA GGA ATT CTG TGC CTG AGC –
Q_{109} E_{110} G_{111} I_{112} L_{113} C_1 L_2 S_3

Figure S28. Construction of pTXB1 αS NpuDnaE-His_6 Plasmids.

DNA Oligomers Used for αS QuikChange® Mutagenesis.

i. Mutation $E_{114}C$ in αS

Forward: 5' – CCCCACAGGAAGGAATTCTGTGCGATATGCCTGTGGATCCTGA – 3'

Reverse: 5' – TCAGGATCCACAGGCATATCGCACAGAATTCCTTCCTGTGGGG – 3'

ii. Mutation $Y_{125}C$ in αS

Forward: 5' – GATCCTGACAATGAGGCTTGCGAAATGCCTTCTGAGGAAG – 3'

Reverse: 5' – CTTCCTCAGAAGGCATTTCGCAAGCCTCATTGTCAGGATC – 3'

iii. Codon optimization C_1L_2 of Npu

Forward: 5' – GTACTCCGTCTCAGAGGTGGTTGCCTGAGCTATGAAACGGAAATATTGAC – 3'

Reverse: 5' – GTCAATATTTCCGTTTCATAGCTCAGGCAACCACCTCTGAGACGGAGTAC – 3'

iv. PacI site introduction between Ub-G_{76} and Npu-C_1

Forward: 5' – CCGTCTCAGAGGTGGTTAATTAAGCCTGAGCTATG – 3'

Reverse: 5' – CATAGCTCAGGCTTAATTAACCACCTCTGAGACGG – 3'

v. PacI site introduction between $αS_{122}$ and Mxe-C_1

Forward: 5' – CTGTGGATCCTGACAATTAATTAAGCATCACGGGAGATG – 3'

Reverse: 5' – CATCTCCCGTGATGCTTAATTAATTGTCAGGATCCACAG – 3'

vi. Deletion of PacI site

Forward: 5' – TGCCTGTGGATCCTGACAATTGCCTGAGCTATG – 3'

Reverse: 5' – CATAGCTCAGGCAATTGTCAGGATCCACAGGCA – 3'

vii. Deletion of $αS_{114-122}$

Forward: 5' – CCCACAGGAAGGAATTCTGTGCCTGAGCTATGAA – 3'

Reverse: 5' – TTCATAGCTCAGGCACAGAATTCCTTCCTGTGGG – 3'

viii. Insertion of $αS_{123-124}$ and deletion of PacI site

Forward: 5' – ATATGCCTGTGGATCCTGACAATGAGGCTTGCCTGAGCTAT – 3'

Reverse: 5' – ATAGCTCAGGCAAGCCTCATTGTCAGGATCCACAGGCATAT – 3'

Figure S29. DNA Oligomers Used for Mutagenesis.

Overexpression and Purification of Full-length αS Cys Mutants (Oxoamide Control Proteins). pRK-αSC_{125} and pRK-αSC_{114} were transformed into competent *E. coli* BL21(DE3) cells using the heat shock method. Single colonies were used to inoculate 4 mL of LB media supplemented with ampicillin (Amp, 100 μg/mL). The primary culture was incubated at 37 °C with shaking at 250 rpm for 4 h. The primary culture was used to inoculate 500 mL of LB media containing Amp (100 μg/mL) which was grown overnight at 37 °C with shaking at 250 rpm. The cells were harvested by centrifugation at 5000 x g for 15 min, and the resulting pellet was re-suspended in lysis buffer (40 mM tris(hydroxymethyl)aminomethane (Tris), 5 mM ethylenediaminetetraacetic acid (EDTA), pH 8.2) supplemented with 1 mM phenylmethanesulfonyl fluoride (PMSF) and 10 units/mL DNase I – Grade II. The cells were lysed by sonication, boiled for 20 min at 100 °C, and centrifuged for 20 min at 14,200 x g at 4 °C. The clear supernatant was dialyzed against purification buffer (20 mM Tris, pH 8.0) overnight at 4 °C. The resulting solution was purified over a HiTrap Q HP column (5 mL) on an ÄKTA FPLC using a 100 min NaCl gradient (0 to 500 mM NaCl in 20 mM Tris, pH 8.0). The fractions containing the product were identified by MALDI MS, pooled, and dialyzed against labeling buffer (20 mM Tris, 100 mM, pH 7.5) overnight. The purified Cys-containing αS proteins (αSC_{125} and αSC_{114}) were quantified by the bicinchoninic acid (BCA) assay (Thermo Scientific Pierce), and stored at – 80 °C until further use. Protein masses are given in Table S3.

Overexpression and Purification of pTXB1-α$S_{1\text{-}113}$Npu-His_6 and pTXB1-α$S_{1\text{-}124}$Npu-His_6. The pTXB1-α$S_{1\text{-}113}$Npu-His_6 and pTXB1-α$S_{1\text{-}124}$Npu-His_6 plasmids were separately transformed into *E. coli* BL21(DE3) cells. Single colonies were picked based on Amp resistance and used to inoculate 4 mL of LB medium containing Amp (100 μg/mL) which was incubated at 37 °C, shaking at 250 rpm for 4 h. The primary culture was then added to 1 L of LB media containing

Amp (100 μg/mL) and incubated at 37 °C, shaking at 250 rpm. When the OD_{600} reached 0.6 – 1.0, the secondary culture was induced with 0.5 mM isopropyl-β-D-thiogalactopyranoside (IPTG) and incubated at 18 °C with shaking at 250 rpm overnight. The cells were harvested from media by centrifugation at 5000 x g for 15 min, and the resulting pellet was suspended in 30 mL of lysis buffer (40 mM Tris, 5 mM EDTA, 5 mM imidazole, pH 8.2) supplemented with protease inhibitor cocktail, 1 mM PMSF and 10 units/mL DNase I – Grade II. Cells were lysed by sonication on ice with 5 cycles of 1 min pulses separated by 1 min rest. After centrifuging the lysate at 14,200 x g for 20 min at 4 °C, the supernatant was incubated with 5 mL Ni-NTA resin for 1 h on ice. After incubation, the slurry was transferred to a fritted column, and the liquid allowed to flow through. The beads were first washed with 10 mL 50 mM 4-(2-hydroxyethyl)-1-piperazineethanesulfonic acid (HEPES), pH 7.5. Then, the beads were successively washed with 6 mL 50 mM HEPES solutions containing 5 mM and 10 mM imidazole. "On column" thiolysis was initiated by the addition of 300 mM sodium 2-mercaptoethanesulfonate (MESNA) in 15 mL 50 mM HEPES, pH 7.5. The column was incubated on a rotisserie at room temperature. After 48 h of incubation, the flow-through was collected and dialyzed against 3 L of 10 mM sodium citrate, pH 5.0 overnight. The dialyzed protein was purified over a HiTrap SP HP column on an ÄKTA FPLC using a 100 min NaCl gradient (0 to 500 mM NaCl in 20 mM sodium citrate, pH 5.0). After analysis by MADLI MS, the fractions containing the thioester product ($\alpha S_{1\text{-}113}$-SR or $\alpha S_{1\text{-}124}$-SR) were pooled and dialyzed against water. After quantification by the BCA assay, the protein was dried using a vacuum centrifuge and stored at -80 °C until further use. Protein masses are given in Table S3.

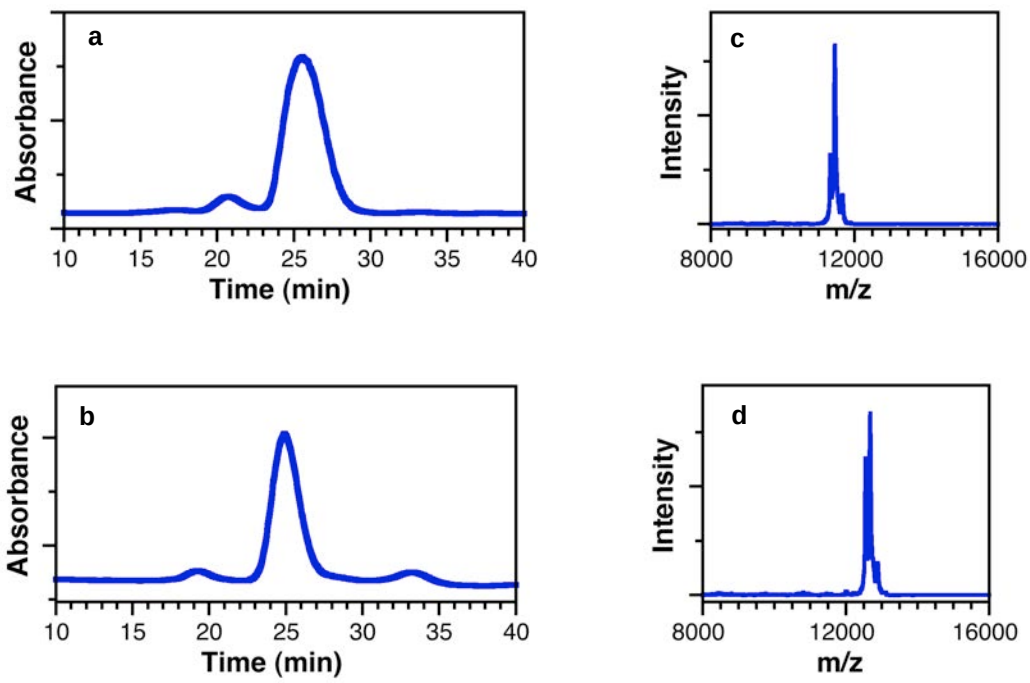

Figure S30. Protein Thioester Purification. FPLC chromatograms (a) $\alpha S_{1\text{-}113}$-SR (b) $\alpha S_{1\text{-}124}$-SR; MALDI MS spectra of (c) $\alpha S_{1\text{-}113}$-SR (d) $\alpha S_{1\text{-}124}$-SR. UV absorbance monitored at 220 nm.

Native Chemical Ligation to form $\alpha SC_{114}E'_{137}$ and $\alpha SC_{125}E'_{130}$. The expressed N-terminal protein thioester fragment ($\alpha S_{1\text{-}113}$-SR or $\alpha S_{1\text{-}124}$-SR, 1.5 equiv; 0.32 μmol) and the C-terminal thiopeptide fragment ($\alpha S_{114\text{-}140}C_{114}E'_{137}$ or $\alpha S_{125\text{-}140}C_{125}E'_{130}$, 1 equiv; 0.21 μmol) were dissolved in 200 μL of freshly prepared, degassed ligation buffer (6 M guanidiumn hydrochloride, 200 mM Na_2HPO_4, 20 mM TCEP, 1% v/v thiophenol, pH 7.2). The reactions were carried out at 37 °C for 7 to 16 h, shaking at 1000 rpm. The ligation was allowed to react until the N-terminal Cys thiopeptide was consumed, and was monitored by MALDI MS. Upon completion, the ligation solution was brought up to 2 mL with Milli-Q water and dialyzed against 20 mM Tris, 100 mM NaCl, pH 7.5 to remove excess ligation buffer reagents.

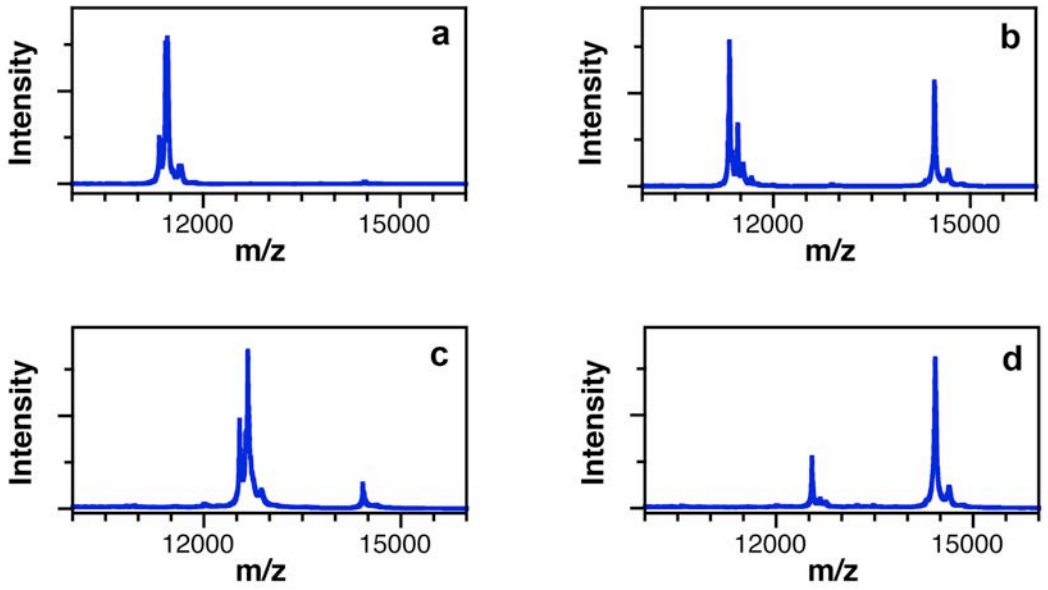

Figure S31. MALDI MS Analysis of NCL Reactions. (a) reaction time = 5 min for $\alpha SC_{114}E'_{137}$, (b) reaction time = overnight for $\alpha SC_{114}E'_{137}$, (c) reaction time = 5 min for $\alpha SC_{125}E'_{130}$, (d) reaction time = 5 h for $\alpha SC_{125}E'_{130}$.

Labeling with Fluorescein Maleimide. For Fam labeling reactions, the amount of ligated thioprotein was calculated assuming a 100% ligation yield relative to N-terminal Cys peptide starting material. Either the dialyzed ligated protein (1 equiv; 0.2 μmol) or the corresponding oxamide control protein was incubated with labeling buffer containing TCEP (10 equiv) for 15 min at room temperature to break any disulfide bonds that formed during the dialysis. After adjusting the protein concentration to 0.5 mg/mL, fluorescein-5-maleimide (10 equiv) was added to the protein from a stock solution in DMSO. The reaction was carried out at 4 °C for 24 h without shaking. The resulting fluorescein-labeled protein was dialyzed against purification buffer (20 mM Tris, pH 8.0) and purified over a HiTrap Q HP column on an ÄKTA FPLC using a 100 min NaCl gradient (0 to 1 M NaCl in 20 mM Tris, pH 8.0). The fractions containing the product were identified by MALDI MS and dialyzed against 20 mM Tris, pH 7.0 – 7.2 overnight, 4 °C prior to HPLC purification. Fam-labeled αS protein (both thio and oxo) eluted

as two separate peaks, one peak as a pure Fam-labeled αS protein and the other peak as Fam-labeled αS protein non-covalently bound to the dye (see, for example, Fig. S35). These two peaks were kept separate during dialysis and HPLC injection. The dialyzed, labeled proteins were further purified by reverse-phase HPLC on a Vydac 218TP C4 semi-prep column using the following gradient: isocratic at 95% aqueous phase for 5 min, and then ranging from 95% to 75% aqueous phase over 5 min, then to 55% over 20 min, then to 0% aqueous phase over 5 min, then returning to 95% aqueous phase during a 5 min wash out period. MALDI MS was used to confirm identities. Following HPLC purification, the product fractions were combined and diluted with water such that CH_3CN concentration was ~15%. Then, the purified protein was concentrated and the buffer was exchanged by centrifugation with a 20 mM Tris, 100 mM NaCl, pH 7.5 using an Amicon (Millipore) Ultra 0.5 mL 3 kDa spin column.

Table S3. Calculated and Observed Protein Masses.

Protein	Calculated m/z $[M+H]^+$	Observed m/z $[M+H]^+$	Calculated m/z $[M+Na]^+$	Observed m/z $[M+Na]^+$
αSC_{114}	14434	14432	14456	-
$\alpha S\psi_{114}$	14862	-	14884	14881
$\alpha S_{1\text{-}113}$-SR	11453	11454	11475	-
$\alpha SC_{114}E'_{137}$	14451	14454	14473	-
$\alpha S\psi_{114}E'_{137}$	14879	-	14901	14902
αSC_{125}	14401	14407	14423	-
$\alpha S\psi_{125}$	14828	-	14850	14854
$\alpha S_{1\text{-}124}$-SR	12666	12669	12688	-
$\alpha SC_{125}E'_{130}$	14417	14420	14439	-
$\alpha S\psi_{125}E'_{130}$	14844	-	14866	14864

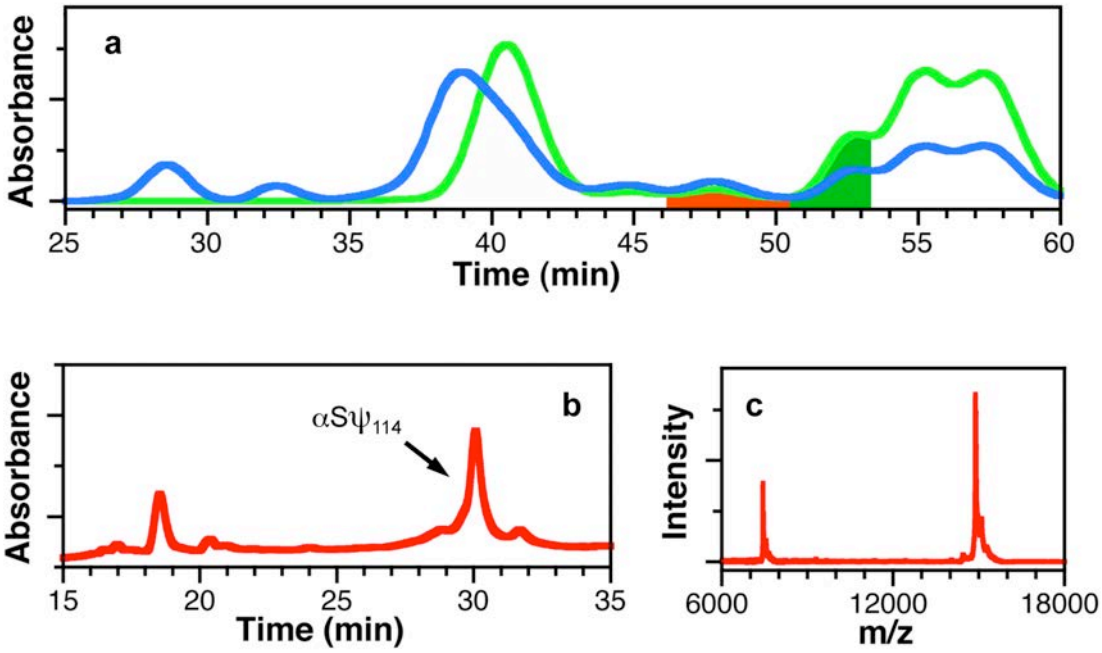

Figure S32. Purification of αSψ$_{114}$ by FPLC Followed by HPLC. (a) FPLC chromatogram (blue: 220 nm, green 488 nm) of αSψ$_{114}$, (b) HPLC chromatogram (444 nm) of αSψ$_{114}$, (c) MALDI MS of αSψ$_{114}$. Peak assignments based on MALDI MS analysis. Red and green coloring indicate FPLC fractions taken on to further purification by HPLC. HPLC purification of the red fraction is shown in (b).

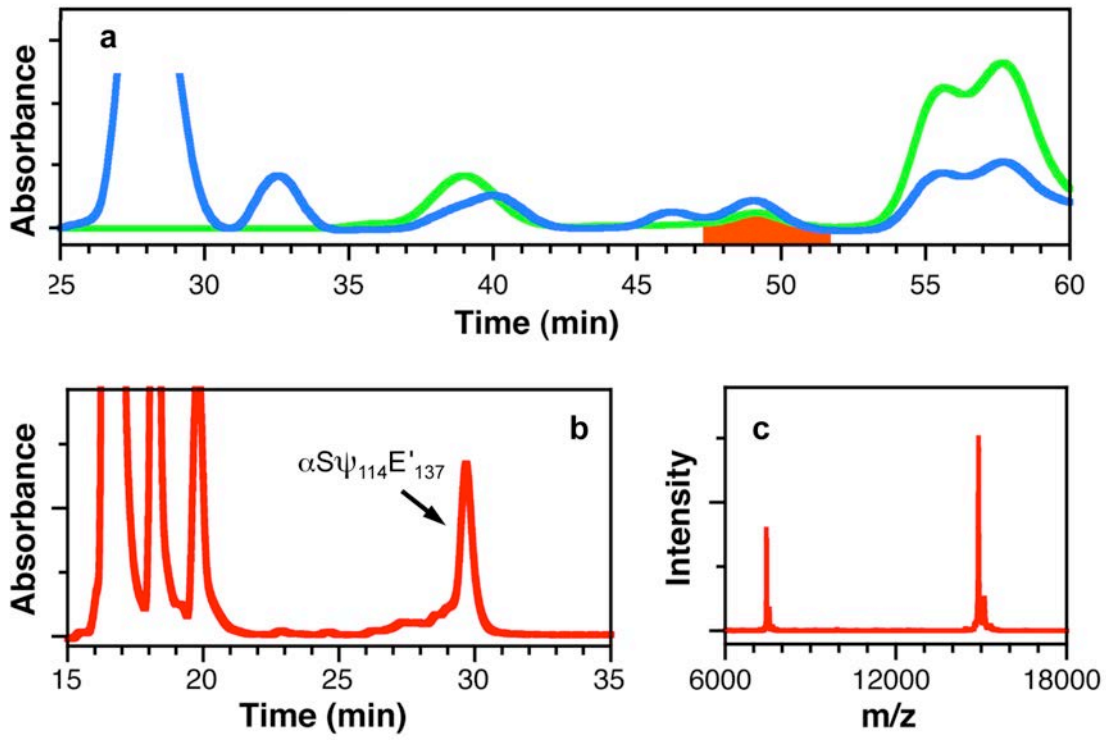

Figure S33. Purification of αSψ$_{114}$E'$_{137}$ by FPLC Followed by HPLC. (a) FPLC chromatogram (blue: 220 nm, green 488 nm) of αSψ$_{114}$E'$_{137}$, (b) HPLC chromatogram (444 nm) of αSψ$_{114}$E'$_{137}$, (c) MALDI MS of αSψ$_{114}$E'$_{137}$. Peak assignments based on MALDI MS analysis. Red coloring indicates FPLC fractions taken on to further purification by HPLC. HPLC purification of the red fraction is shown in (b).

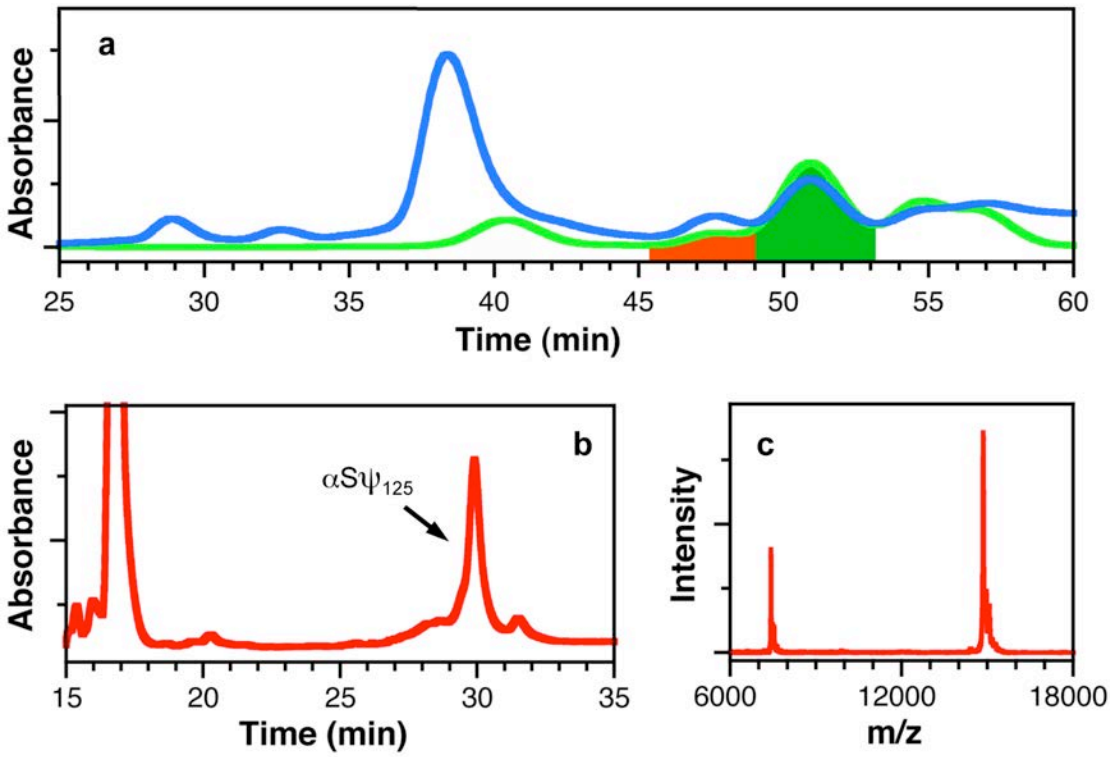

Figure S34. Purification of αSψ$_{125}$ by FPLC Followed by HPLC. (a) FPLC chromatogram (blue: 220 nm, green 488 nm) of αSψ$_{125}$, (b) HPLC chromatogram (444 nm) of αSψ$_{125}$, (c) MALDI MS of αSψ$_{125}$. Peak assignments based on MALDI MS analysis. Red and green coloring indicate FPLC fractions taken on to further purification by HPLC. HPLC purification of the red fraction is shown in (b).

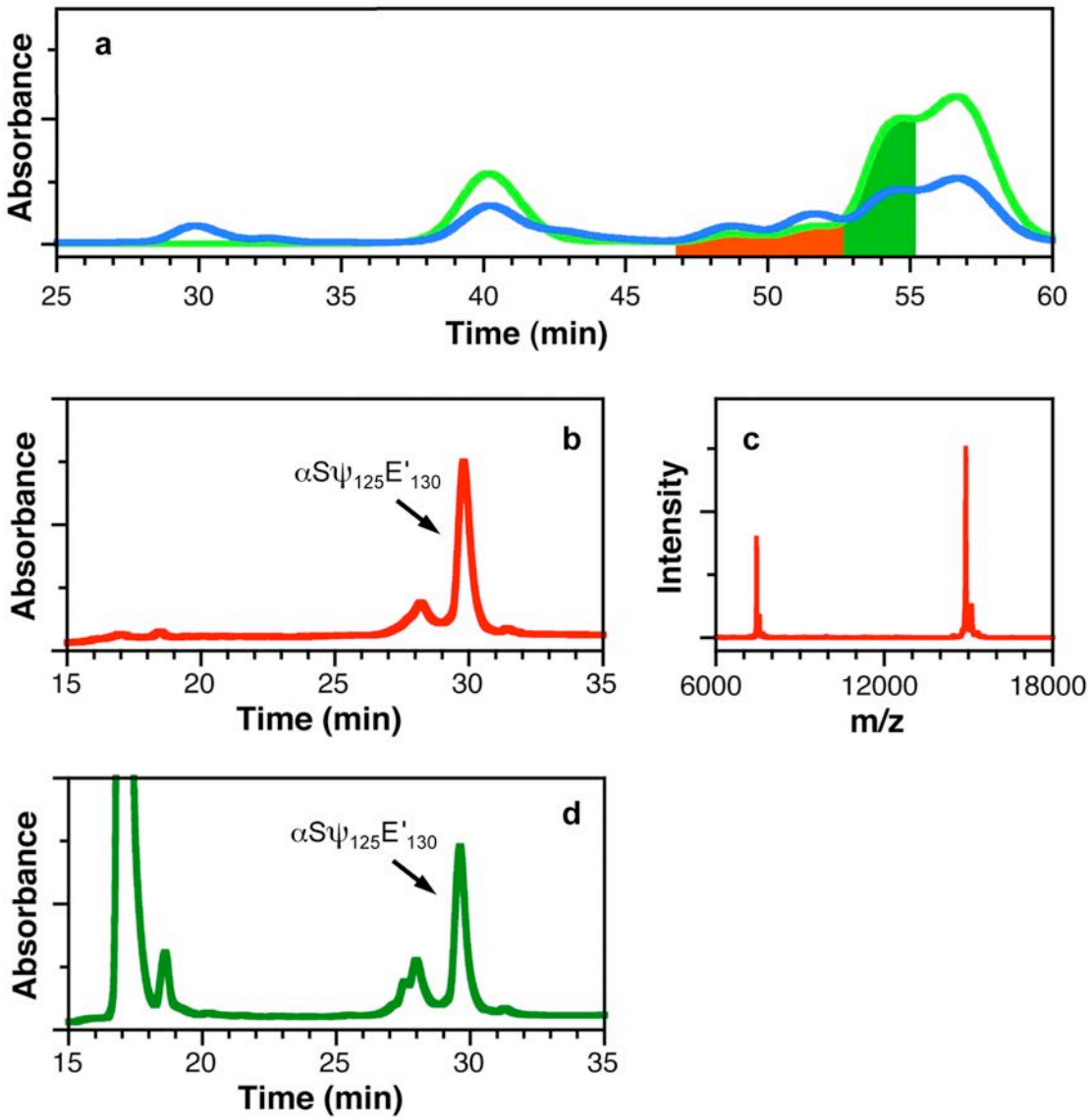

Figure S35. Purification of αSψ$_{125}$E'$_{130}$ by FPLC Followed by HPLC. (a) FPLC chromatogram (blue: 220 nm, green 488 nm) of αSψ$_{125}$E'$_{130}$, (b) HPLC chromatogram (444 nm) of αSψ$_{125}$E'$_{130}$, (c) MALDI MS of αSψ$_{125}$E'$_{130}$, (d) HPLC chromatogram (444 nm) of αSψ$_{125}$E′$_{130}$. Peak assignments based on MALDI MS analysis. Red and green coloring indicate FPLC fractions taken on to further purification by HPLC. HPLC purification of the red fraction is shown in (b). HPLC purification of the green fraction is shown in (d). Peak at 17 min corresponds to free Fam-maleimide dye.

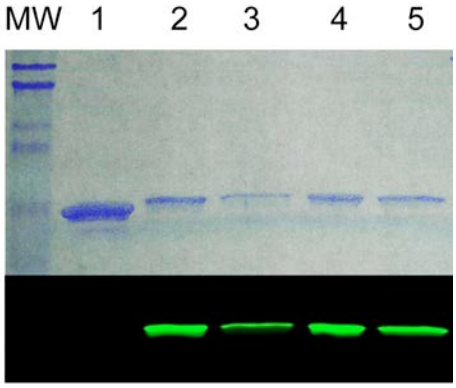

Figure S36. PAGE Gel Analysis of Labeled αS Constructs. Lanes: MW) Molecular weight markers (kDa), 17, 25, 32, 47, 80; 1) αS WT; 2) $\alpha S\psi_{114}E'_{137}$; 3) $\alpha S\psi_{114}$; 4) $\alpha S\psi_{125}E'_{130}$; 5) $\alpha S\psi_{125}$. Top: Coomassie staining, Bottom: fluorescence imaging. Gel imaged using a Typhoon FLA 7000, fluorescence was detected using 473 nm excitation and a Y520 filter, using a 100 µm pixel size.

αS Refolding Assays. Tris buffers (20 mM Tris, 100 mM NaCl, pH 7.5) containing trimethylamine oxide (TMAO) were prepared such that upon addition of protein (absorbance of final solution at 492 nm was between 0.11 and 0.07, corresponding to 1.47 - 1.07 μM), the final TMAO concentrations were 0 M, 2 M, and 4 M.[5] Fluorescence lifetimes were measured immediately following sample dilution in TMAO (to a final volume of 125 μL).

αS Fluorescence Lifetime Measurements. Time-resolved fluorescence measurements were made on solutions of labeled αS proteins in TMAO using the TCSPC method on a Photon Technologies International QuantaMaster™ 40 system with a B&H PMH-100 detector (PTI; Piscataway, NJ, USA). The samples were excited using a 486 nm pulsed light-emitting diode (LED) operating at 250 KHz. Emission was monitored at 520 nm. Data analysis was performed with FelixGX software using the "1 to 4 Exponential Lifetime" model to develop fits based Equations S2 and S3 and calculate residuals according to Equation S4 in a manner identical to that described above for the small molecules. Lifetime decays of all of the αS variants could be fit using a single-exponential model (Eq. S2, n = 1) in 0 and 2M TMAO. For the 4M TMAO samples, a bi-exponential model (Eq. S2, n = 2) was more appropriate as judged by χ^2 analysis and inspection of the weighted-residual plots. This allowed us to calculate intensity weighted average lifetimes that were used in determining E_Q as described in the main text. Representative fits and the corresponding residual plots for the $\alpha S\psi_{114}E'_{137}$/ $\alpha S\psi_{114}$ and $\alpha S\psi_{125}E'_{130}$/ $\alpha S\psi_{125}$ pairs are shown in Figures S38 – S39. Table S4 contains the corresponding lifetime parameters and χ^2-analyses.

The determination of uncertainty in a composite function such as the average lifetime can be complicated, particularly when the component lifetimes may be similar. In this case, the relatively wide instrument response function (shown in Figures S37 – S39), contributes to the

uncertainty in the individual components of the bi-exponential lifetime fits. Therefore, to determine confidence intervals of the average lifetimes, we used an approach described by Lakowicz in which we fixed one of the two component lifetimes to a limiting value and refit the data, optimizing the other parameters.[19] For example, to determine the upper limit for the average lifetime of $\alpha S\psi_{114}E'_{137}$ in 4 M TMAO, we fixed the longer component lifetime (τ_1) at 3.348 ns + 0.246 ns = 3.594 ns, and re-optimized the bi-exponential fit, obtaining an average lifetime of 2.024 ns, which we report as the upper bound of the average lifetime for $\alpha S\psi_{114}E'_{137}$ in 4 M TMAO. Similarly, we fixed the shorter component lifetime (τ_2) at 1.721 ns - 0.079 ns = 1.642 ns, and re-optimized the bi-exponential fit, obtaining an average lifetime of 1.969 ns, which we report as the lower bound of the average lifetime for $\alpha S\psi_{114}E'_{137}$ in 4 M TMAO. Fixing any of the other single parameters at their limiting values did not give values outside of these upper or lower bounds. Thus, although the data do not allow us to determine the individual parameters with high levels of certainty, the uncertainty in the average lifetime is relatively small, consistent with the goodness-of-fit observed in the reduced χ^2 values.

Quenching efficiencies, $E_Q(\tau)$, were calculated according to Equation S5 where τ_{Thio} is the lifetime of the thioamide-labeled version of αS and τ_0 is the lifetime of the oxoamide control. Since the lifetimes of the proteins in 4 M TMAO were determined with asymmetric confidence intervals as described above, we chose to determine confidence intervals in the $E_Q(\tau)$ values using the bounding values of the average lifetimes. Confidence intervals for $E_Q(\tau)$ were determined by 1) calculating $E_Q(\tau)$ using the upper bound of τ_{Oxo} and the lower bound of τ_{Thio} to determine the upper bound of $E_Q(\tau)$; and 2) calculating $E_Q(\tau)$ using the lower bound of τ_{Oxo} and the upper bound of τ_{Thio} to determine the lower bound of $E_Q(\tau)$. Table S5 contains the values of

$E_Q(\tau)$ and the associated confidence intervals for each thioamide protein construct in 0, 2, or 4 M TMAO.

Measurements of the lifetime of Fam-Cys (**17**) alone in 0, 2, and 4 M TMAO buffer showed no significant change in fluorescence lifetime (4.048 ± 0.007, 3.997 ± 0.006, and 3.937 ± 0.007 ns, repectively). These data are shown in Figure S37.

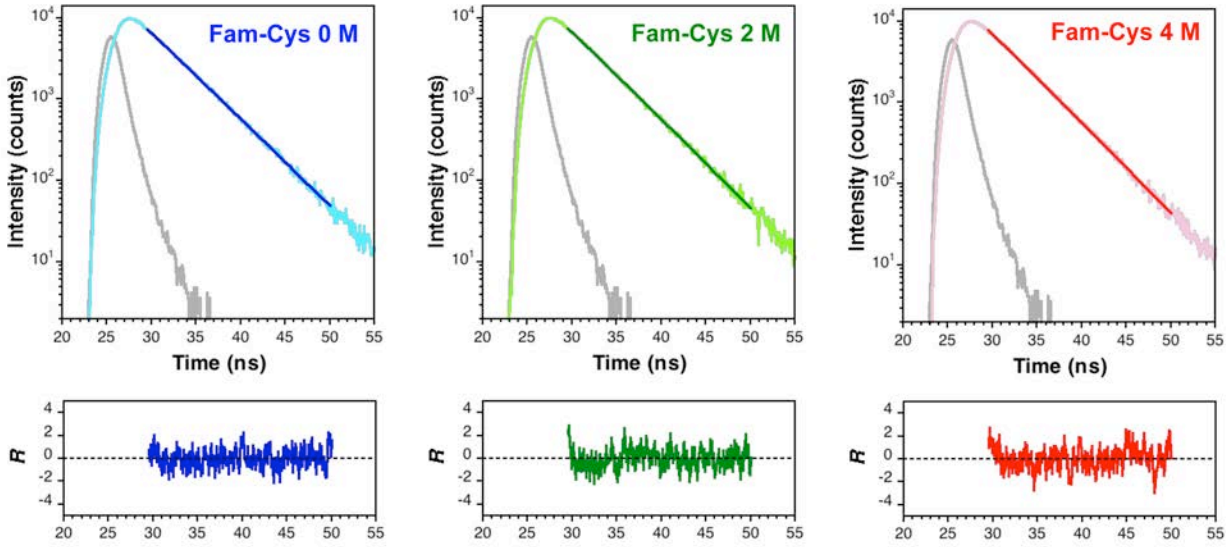

Figure S37. TMAO Solutions of Fam-Cys (ψ, **17**). Single exponential fits and weighted residuals of fluorescence lifetime measurements of approximately 1 μM Fam-Cys in Tris buffer with 0, 2, or 4 M TMAO. The instrument response function is shown in gray.

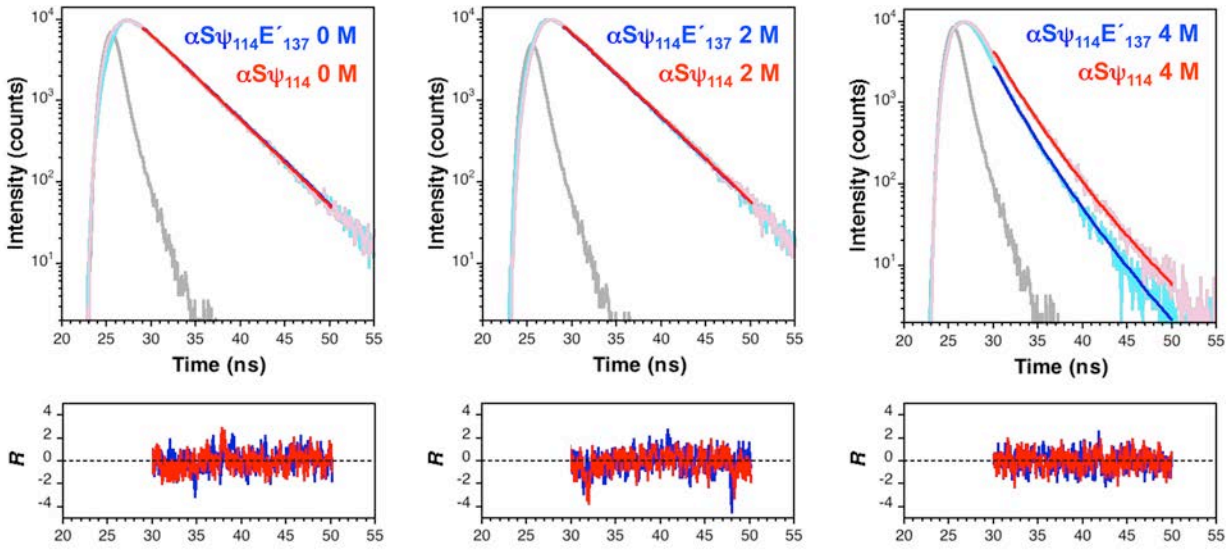

Figure S38. TMAO Refolding of $\alpha S\psi_{114}E'_{137}$. Bi-exponential fits and weighted residuals of fluorescence lifetime measurements of approximately 1 μM $\alpha S\psi_{114}E'_{137}$ or $\alpha S\psi_{114}$ in Tris buffer with 0, 2, or 4 M TMAO. The instrument response function is shown in gray.

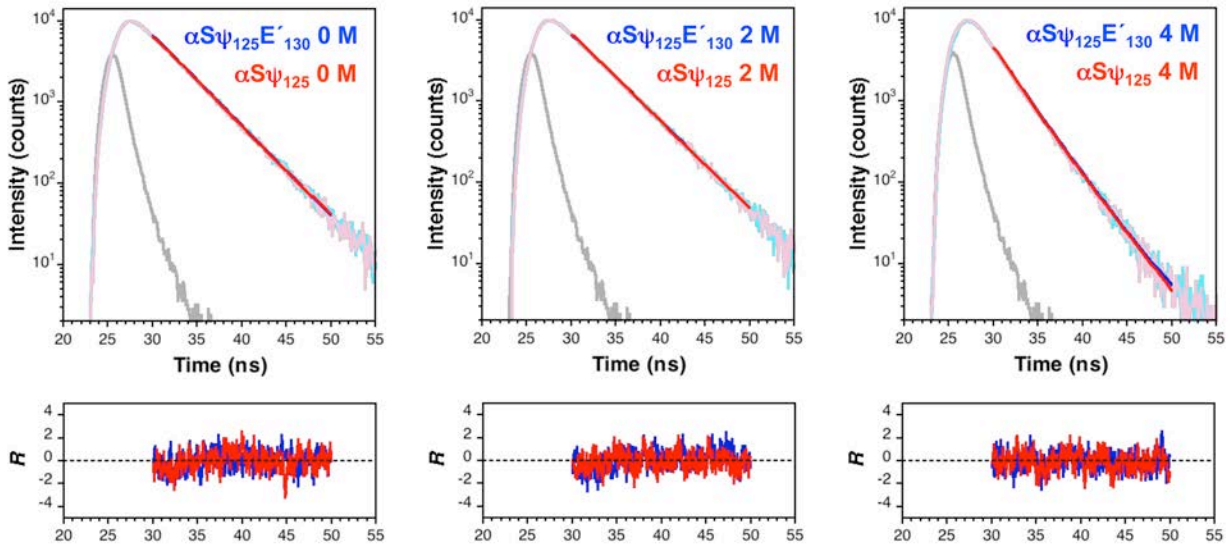

Figure S39. TMAO Refolding of $\alpha S\psi_{125}E'_{130}$. Bi-exponential fits and weighted residuals of fluorescence lifetime measurements of approximately 1 μM $\alpha S\psi_{125}E'_{130}$ or $\alpha S\psi_{125}$ in Tris buffer with 0, 2, or 4 M TMAO. The instrument response function is shown in gray.

Table S4. Fluorescence Lifetime Parameters from aS TMAO Refolding Assays.

Protein - [TMAO]	τ_{Avg}[a] (ns)	τ_1 (ns)	A_1	τ_2 (ns)	A_2	χ^2
$\alpha S\psi_{114}E'_{137}$ - 0 M	-	4.155 ± 0.011	0.874 ± 0.004	-	-	1.004
$\alpha S\psi_{114}$ - 0 M	-	4.162 ± 0.009	0.887 ± 0.003	-	-	1.073
$\alpha S\psi_{114}E'_{137}$ - 2 M	-	4.122 ± 0.011	0.864 ± 0.004	-	-	1.074
$\alpha S\psi_{114}$ - 2 M	-	4.121 ± 0.009	0.889 ± 0.004	-	-	0.869
$\alpha S\psi_{114}E'_{137}$ - 4 M	2.003 (1.969 – 2.024)	3.348 ± 0.246	0.119 ± 0.045	1.721 ± 0.079	1.102 ± 0.037	0.887
$\alpha S\psi_{114}$ - 4 M	2.462 (2.412 – 2.487)	3.376 ± 0.299	0.267 ± 0.129	1.967 ± 0.196	0.846 ± 0.075	0.866
$\alpha S\psi_{125}E'_{130}$ - 0 M	-	3.804 ± 0.011	0.931 ± 0.004	-	-	1.097
$\alpha S\psi_{125}$ - 0 M	-	3.835 ± 0.011	0.929 ± 0.005	-	-	0.916
$\alpha S\psi_{125}E'_{130}$ - 2 M	-	3.965 ± 0.011	0.915 ± 0.004	-	-	0.996
$\alpha S\psi_{125}$ - 2 M	-	3.986 ± 0.011	0.905 ± 0.004	-	-	0.863
$\alpha S\psi_{125}E'_{130}$ - 4 M	2.479 (2.411 – 2.517)	3.102 ± 0.227	0.466 ± 0.204	1.881 ± 0.289	0.800 ± 0.121	0.953
$\alpha S\psi_{125}$ - 4 M	2.465 (2.365 – 2.475)	2.949 ± 0.089	0.645 ± 0.101	1.594 ± 0.222	0.729 ± 0.059	0.944

[a] Confidence interval for τ_{Avg} determined by refitting to a biexponential model with τ_1 or τ_2 fixed to upper or lower bound of the uncertainty of these component lifetimes.

Table S5. Quenching Efficiency from aS TMAO Refolding Assays.

Protein - [TMAO]	$E_Q(\tau)$[a]
$\alpha S\psi_{114}E'_{137}$ - 0 M	0.002 (-0.003 – 0.007)
$\alpha S\psi_{114}E'_{137}$ - 2 M	0.002 (-0.005 – 0.005)
$\alpha S\psi_{114}E'_{137}$ - 4 M	0.186 (0.161 – 0.208)
$\alpha S\psi_{125}E'_{130}$ - 0 M	0.008 (0.003 – 0.014)
$\alpha S\psi_{125}E'_{130}$ - 2 M	0.005 (0.000 – 0.011)
$\alpha S\psi_{125}E'_{130}$ - 4 M	-0.006 (-0.064 – 0.026)

[a] Confidence interval for $E_Q(\tau)$ determined by calculating $E_Q(\tau)$ using the upper bound of τ_{Oxo} and the lower bound of τ_{Thio} to determine the upper bound of $E_Q(\tau)$; and calculating $E_Q(\tau)$ using the lower bound of τ_{Oxo} and the upper bound of τ_{Thio} to determine the lower bound of $E_Q(\tau)$.

References

(1) Wagner, A. M.; Fegley, M. W.; Warner, J. B.; Grindley, C. L. J.; Marotta, N. P.; Petersson, E. J. *J. Am. Chem. Soc.* **2011**, *133*, 15139-15147.
(2) Kitamura, N.; Fukagawa, T.; Kohtani, S.; Kitoh, S.-i.; Kunimoto, K.-K.; Nakagaki, R. *J. Photochem. Photobiol.* **2007**, *188*, 378-386.
(3) Lin, S.; Struve, W. S. *Photochem. Photobiol.* **1991**, *54*, 361-365.
(4) Spence, M. T. Z.; Johnson, I. D. *The molecular probes handbook : a guide to fluorescent probes and labeling technologies*; Life Technologies Corporation: [Carlsbad, CA], 2010.
(5) Huang, D.; Robison, A. D.; Liu, Y.; Cremer, P. S. *Biosens. Bioelectron.* **2012**, *38*, 74-78.
(6) Guha, S. N.; Mittal, J. P. *J. Photochem. Photobiol.* **1995**, *92*, 181-188.
(7) Eastman Kodak, C. *Kodak optical products*; Eastman Kodak Co.: Rochester, N.Y., 1991.
(8) Mujumdar, R. B.; Ernst, L. A.; Mujumdar, S. R.; Lewis, C. J.; Waggoner, A. S. *Bioconj. Chem.* **1993**, *4*, 105-111.
(9) Chenlo, F.; Moreira, R.; Pereira, G.; Vazquez, M. a. J. *J. Chem. Eng. Data* **1996**, *41*, 906-909.
(10) Bondi, A. *J. Phys. Chem.* **1964**, *68*, 441-451.
(11) Evnin, L. B.; Vasquez, J. R.; Craik, C. S. *Proc. Natl. Acad. Sci. USA* **1990**, *87*, 6659-6663.
(12) Erlanger, B. F.; Cohen, W.; Kokowsky, N. *Arch. Biochem. Biophys.* **1961**, *95*, 271-&.
(13) Inagami, T. *J. Biol. Chem.* **1969**, *66*, 277-279.
(14) Grant, G. A.; Eisen, A. Z. *Biochemistry* **1980**, *19*, 6089-6095.
(15) Shalaby, M. A.; Grote, C. W.; Rapoport, H. *J. Org. Chem.* **1996**, *61*, 9045-9048.
(16) Culik, R. M.; Jo, H.; DeGrado, W. F.; Gai, F. *J. Am. Chem. Soc.* **2012**, *134*, 8026-8029.
(17) Shah, N. H.; Dann, G. P.; Vila-Perello, M.; Liu, Z. H.; Muir, T. W. *J. Am. Chem. Soc.* **2012**, *134*, 11338-11341.
(18) Wissner, R. F.; Batjargal, S.; Fadzen, C. M.; Petersson, E. J. *J. Am. Chem. Soc.* **2013**, *135*, 6529-6540.
(19) Lakowicz, J. R. *Principles of fluorescence spectroscopy*; Springer, 2006.